博士論文 (要約)

Time budget and activity pattern of humpback whales, *Megaptera novaeangliae*, in the Northern foraging grounds

(北方採餌海域におけるザトウクジラの行動時間配分と活動様式)

2018 年度

東京大学大学院　新領域創成科学研究科　自然環境学専攻

秋山　優

指導教員　東京大学大気海洋研究所　佐藤克文

Table of contents

CHAPTER 1

General introduction

1.1. Life history of humpback whales

1.1.1. Lifespan and seasonal migration

The majority of marine mammals, such as whales, dolphins and porpoises belong to the order Cetacea and there are two major group of extant whales. One is Odontoceti, the toothed whales which are more diverse, with approximately 76 known species, and another is Mysticeti, the baleen whales with approximately 14 known species (Berta 2015), which has plates of baleen growing from the roof of its mouth instead of teeth, (Berta et al. 2005). Humpback whales (*Megaptera novaeangliae*) are so named from the distinctive hump of their dorsal fin, and are large baleen whales belonging to family Balaenopteridae, commonly called the rorqual whales.

Humpback whales are widely distributed in oceans all over the world with 14 distinct populations reported to date (Fig. 1-1: NOAA 2016a). Their annual cycle can be divided into two big parts with a distinct geographical and temporal separation. During the spring and summer seasons they are found in foraging grounds at high latitude and when humpback whales are away from the foraging ground, they reduce the energy intake or completely stop feeding (Clapham 1996; Berta et al. 2005). In late autumn after they have stored enough energy, they start a long migration to low latitude breeding grounds where they mate and calve during the winter season (Berta et al. 2005). The distance of annual migration varies with populations and individuals, and still remains unclear for the most parts but the longest migration record to date is approximately 9800 km, identified from

a humpback whale moving between the two breeding areas at Brazil to Madagascar (Stevick et al. 2011). However, this is likely to be underestimated because it does not include the migration to the high latitude foraging ground. Male humpback whales sing a long complex song during the breeding season and it seems that the main purpose of this behavior is to attract the potential mate (Payne and McVay 1971). Females give birth to calves at tropical waters every two to three-year intervals and the duration of gestation is 11 to 12 months (Clapham and Mayo 1987; Clapham 1996; Pierre-Henry 2007). The body length of newborn calves are approximately four meters at birth. They take up at least 43 kg of milk daily and start weaning at about five to six months old and attain independence in about a year old (Pierre-Henry 2007). The social organization of humpback whales are small and unstable both at foraging grounds and breeding grounds although big group can be temporary formed at foraging grounds (Whitehead 1983; Weinrich 1991; Clapham 1996; Valsecchi et al. 2002). Humpback whales attain sexual maturity when they reach about 11 to 12 meter in body length at around the age of five years old. They eventually grow up to about 12 to 16 meters, weighing about 25 to 30 tons with female being approximately one meter larger than male and perhaps live up to 50 to 100 years (Pierre-Henry 2007).

While seasonal migration is known to be their typical annual cycle, there has been an argument recently that some humpback whales do not overwinter in the high latitude. The extent of this phenomenon is unclear, although humpback whales have been observed in foraging grounds during winter and the population in Norway from this study is one example. However, it is known

that these whales in Norway do undergo migration between high latitude and low latitude as there is a report that one whale observed at Norway on January was observed at low latitude few months later (personal communication from researcher in Norway). These may be a new findings of humpback whales from increased study or a consequence of climate change causing shift in timing of migration.

1.1.2. Current status of humpback whales

Due to massive overexploitation in the past, population size of humpback whales was greatly reduced, some by more than 95% of the initial population size (NOAAa 2016). Whales are still being exploited, although, the number of catches has been strictly regulated and population of humpback whales shows a recover. In 2016, the U.S. government announced that most of the humpback populations has been removed from the endangered species list. According to the National Oceanic and Atmosphere Administration (NOAA), currently, of the 14 distinct population, four are still protected as endangered and one is listed as threatened (Fig. 1-1: NOAA 2016a).

Human association with the whales still continues. In coastal areas where whales are easily observed, whale watching is becoming an important industry to draw tourists to countries. Moreover, human activities have addressed new threats such as entanglement to fishing gears, vessel strikes and vessel-based harassment, chemical and noise pollution and climate change (Rus 2002; Berta et al. 2005). Continuous management and conservation act are needed to solve these problems and to enable a sustainable relationship between human and whales.

1.2. Objective of this study

Life of almost all animals can be divided into two behavioral state; the activity state and the rest state (Halle and Stenseth 2000). During activity state animals have tasks which needs to be performed for their survival and reproductive success, and the two important tasks are foraging and breeding. Rest state is the opposite of activity state which may not exactly involve tasks, but animals cannot survive without sufficient amount of rest (Shaw et al. 2002; Lyamin et al. 2008), therefore; is an important part of life.

For humpback whales that generally cease feeding during the migration and breeding period, the success of their survival and reproduction depend largely on energy store during the foraging period (Berta et al. 2005). This thesis, therefore; will specifically focus on behavior of humpback whales during the foraging period. Time and resource are limited for all animals but animal with such an extreme restriction as humpback whales are rare, therefore; understanding the behavior and time budget of such animal is important as they can help us identify the dominant factor which determines the activity pattern and how it affects the survival of wild animals.

The big goal for humpback whales during the foraging period is to store enough energy. Thus, the most important behavior will be foraging, but resting cannot be eliminated. If these two activities can be done at the same spot without moving, that can save time and energy but unfortunately, they need to move, perhaps for better prey or to find the right place to rest. Therefore, within a given 24 hours or approximately 120 days during the foraging period, humpback whale must allocate its time between foraging, moving and resting to accomplish its goal. However, just performing these

activities will not guarantee their fitness. If the activates are not performed the right way, it will be a cost. Therefore, animals should have an adaptive strategy for each activity and do the right thing at the right time, the right way (Halle and Stenseth 2000). Although, quantitative analysis of these behavior on large wild marine mammals like humpback whales have been especially difficult because most activities take place underwater where direct observation is nearly impossible (Doniol-Valcroze et al. 2011; Watanabe et al. 2014; Hazen et al. 2015; Foo et al. 2016; Tyson et al. 2016). Great progress has been made over the last couple of years, with respect to the development of methods using electronic tags, that has enabled us to observe the behavior of animals underwater. Therefore, the objective of this study is to quantitatively address the adaptive strategy of foraging, resting and moving, as well as how humpback whales in the northern foraging grounds allocate time between these activities using accelerometer and video-logger directly attached to humpback whales. In chapter two, foraging behavior of humpback whales in response to change in prey density in a single dive was tested and the efficiency of each foraging dive was calculated. Furthermore, the effect of competitors during foraging events were also investigated by detecting the presence of other animals around the tagged whales using the video-logger. In chapter three, resting characteristics of humpback whales, specifically their resting posture and resting site (depth) selection were quantitatively addressed. In chapter four, time budget and activity pattern of humpback whales foraging in three different foraging grounds, Norway, Iceland and Canada were identified and compared to see how humpback whales of different foraging locations allocate time over various

activities to optimize their fitness. In chapter five, experimental study was conducted to investigate the effect of wave drag on moving cetacean using a trained bottlenose dolphin as to further understand the depth selection of wild humpback whales while moving. Finally, in the last chapter, results from all chapters are summarized and discussed.

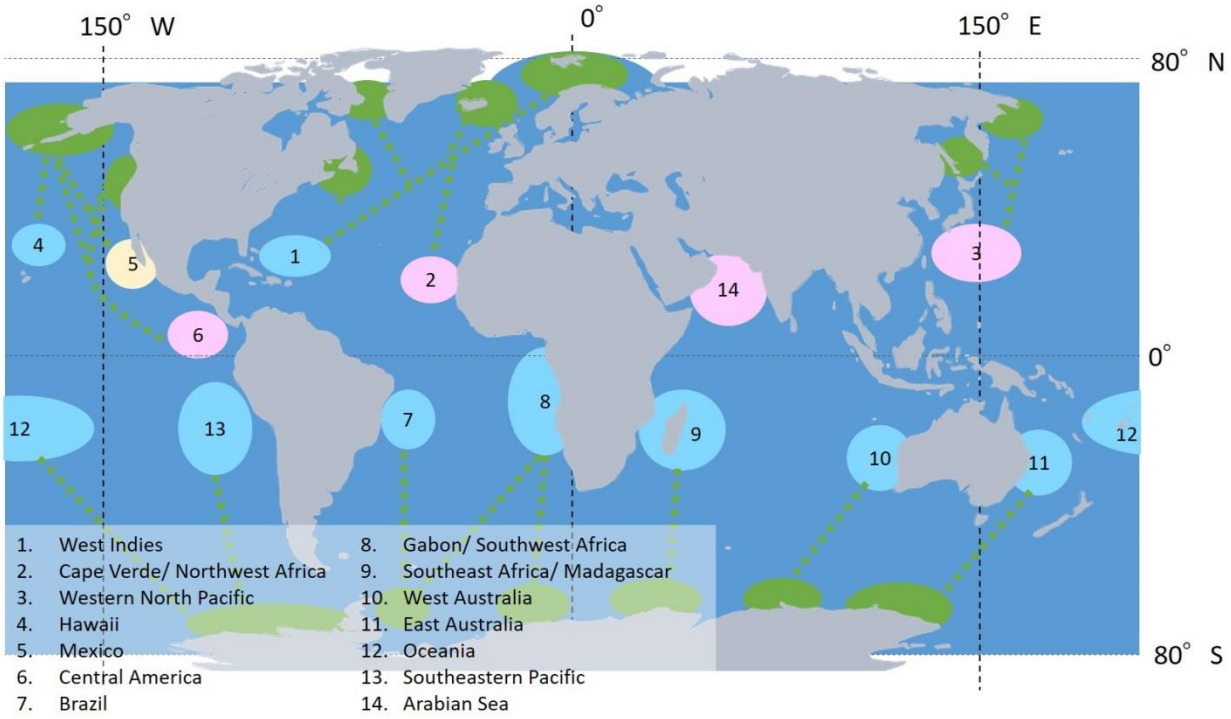

Figure 1-1. Map showing the 14 distinct population of humpback whales and their status. Blue area is the distribution range, green areas are their foraging grounds, light-blue circles are the populations categorized as not at risk, yellow is the threatened, and pink are endangered population (Figure redrawn from NOAAb website).

CHAPTER 2

Adaptive foraging strategies of the Icelandic humpback whales

2.1. Background

Among the diving predators, rorqual whales (*Balaenopteridae*) are the largest predators on earth and their magnificent body size has led to unique characteristics in the contexts of foraging ecology. Rorquals whales (Balaenopteridea), such as blue whales, fin whales and humpback whales, have reduced tough and a series of longitudinal grooves of highly extensible, elastic blubber located on the ventral side of the body (Orton and Brodie 1987; Goldbogen et al. 2007; Goldbogen et al. 2008). This characteristic enables them to perform a unique feeding strategy only seen among rorqual whales, known as lunge feeding. During lunge feeding, they first accelerate to a high speed towards a patch of prey in a burst by energetically rapid fluke stroke (Goldbogen 2007; Goldbogen 2008; Simon et al. 2012). At maximum velocity or just prior, they lower its mandible at wide angle inflating the buccal cavity with the oncoming flow and engulfs a mass of water together with the prey (Fig. 2-1A) and water is pushed out using its tongue and expelled through baleen plates that act as filters to retain prey (Fig. 2-1B: Berta et al. 2005).

Rorqual whales, especially the humpback whales are known to carry out various types of lunge feeding strategy which are unique among population and specialized for specific prey (Weinrich et al. 2009). Some of the commonly addressed types of lunge feeding are bubble-cloud (net) feeding (Fig. 2-2A), vertical lunge feeding (Fig. 2-2B) and lateral lunge feeding (Fig. 2-2C), which can occur both

at surface and underwater. The most common and simplest form of feeding type is the vertical lung feeding where the whale dives and charge into a patch of prey with its mouth open from below at a vertical angle (Fig. 2-2B). Although the most famous and expected feeding type is the bubble-cloud feeding (Fig. 2-2A). This is often seen with several individuals cooperating, therefore; makes a strong visual impression to people. As one produces clouds or net of bubbles, confused prey clumps into middle, then the other whale dives and lunge into the school of prey. Lastly, during lateral lunge feeding, the whale takes a lateral position and swim with its mouth open for 10 to 15 seconds (Fig. 2-2C: Acevedo et al. 2011). Because humpback whales have such diverse adaptation to efficiently capture its prey, identifying the prey item and the type of lunge feeding strategy used is the first step when studying their foraging behavior.

Types of lunge feeding is one of the adaptations for humpback whales to efficiently capture its prey. Another important thing for humpback whales is to modify their foraging behavior to efficiently exploit prey whose density and availability dynamically changes over time. While most carnivores target and capture a single prey at a time, humpback whales forage on densely aggregated krill or schooled fish. Hence, a single engulfment during lunge may induce a drastic decrease in prey density in a single dive (patch), and the decision whether to leave or stay at the prey patch in response to this drastic change should have a significant effect on prey exploitation efficiency. However, whether humpback whales show adaptive behavior in response to the diminishing prey density in a single dive has been technically difficult to test.

Foraging behavior of rorqual whales in relation to prey density was previously studied by attaching multi-sensor digital archival tags onto whales, in combination with prey distribution data measured using ship-mounted echo-sounders (Hazen et al. 2015; Friedlaender et al. 2016b). This method succeeded in providing many fruitful insights on the whales' foraging strategy across patches, but the spatiotemporal resolution was not high enough to detect the change in prey density on a single-dive scale. In this study, relative prey density around humpback whales were estimated at high temporal resolution using a video logger attached to the whales. Moreover, this video-based method enabled to detect the presence of other whales that may potentially affect the foraging behavior of the whale. In nature, predator distribution is linked with prey aggregation, and predators gather in areas of high prey density (Nowacek et al. 2011). Encounters with other animals might be disadvantageous if they increase the competition and risk of predation. Alternatively, such encounters might be advantageous if individuals benefit from the food herded by other animals or cooperate to capture prey, although this was also never tested again due to technical difficulties.

Thus, in this chapter, foraging characteristics of humpback whales in the study site was first distinguished. Secondly, investigated the foraging behavior of humpback whales in response to change in prey density in a single dive and calculated the efficiency of each foraging dive and lastly, identified how humpback whales adjust their foraging duration in response to presence/absence of other individuals.

2.2. Materials and methods

2.2.1. Field study and equipment

Tagging was conducted in Skjálfandi Bay off Húsavík in northern Iceland (66°05'N, 17°19'W; Fig. 2-3), which is known as a feeding ground for many cetaceans (Rasmussen 2009; Akamatsu et al. 2014), from 31 May to 10 June in 2013, and 21 June to 30 June in 2014. Humpback whales were approached slowly, and tags were deployed from a Zodiac inflatable boat (60-hp engine, 5-m long), using an 8-m carbon fiber pole with a tag set at the tip of the pole. Another boat was standing by for safety and to obtain photo-identification records of the whales. The tag was attached to the whale with a suction cup, which naturally detached after a few hours, and was retrieved using its VHF signal.

The animal-borne tag consisted of (1) an accelerometer sensor, W1000-3MPD3GT (26 mm in diameter, 175 mm in length, 140 g in air; Little Leonardo Corp., Tokyo, Japan), programmed to record tri-axial acceleration at 32 Hz; speed, depth, temperature, and tri-axial magnetometer sensors sampling at 1 Hz; (2) a video logger, DVL 400 (23 mm in diameter, 114 mm in length, 80 g in air, for 5 h of recording, 80° field-of-view on land; Little Leonardo Corp.), used in 2013, or DVL 400L (23 mm in diameter, 145 mm in length, 115 g in air, for 10 hours of recording, 80° field-of-view on land; Little Leonardo Corp.), used in 2014; (3) a suction cup (85 mm in diameter; Canadian Tire Corporation, Toronto, Canada); and (4) a VHF radio transmitter (10 mm in height, 10 mm in width, 55 mm in length, 22 g in air; Advanced Telemetry Systems, Isanti, MN, USA), all assembled in one

float (Fig. 2-4)

2.2.2. Body angle alignment

The orientation of the tagged animal can be obtained from tri-axial acceleration and tri-axial magnetism data (Fig. 2-5). However, these signals are expressed in terms of the Euler angles, pitch, roll, and heading with respect to the fixed (Earth) frame (Johnson & Tyack 2003). If the tag is aligned with the body's frame, the whale's orientation can obtain. This is rarely the case since the tag is attached using a pole; therefore, the tag's frame had to be adjusted with respect to the body's frame. Time-series data obtained from the accelerometers were adjusted using MATLAB R2013a Student Version, following the method of Johnson and Tyack (Johnson & Tyack 2003), which first obtains angular measurements of the orientation of the tag on the whale, then deducts the whale frame angles from the obtained angles.

2.2.3. Stroke and pitch angle calculation from acceleration

The compensated data were used to obtain swimming stroke and pitch angle using IGOR Pro (WaveMetrics, Lake Oswego, OR, USA) following the method of Tanaka et al. (2001) and Sato et al. (2003). The acceleration data were separated to low-frequency gravity-based acceleration using the 0.1 Hz low-pass filter in the IFDL software in IGOR Pro. By subtracting this gravity-based acceleration from the original, high-frequency acceleration was obtained, reflecting the propulsive (stroking) activity. The value of low-pass filtering was determined as 0.1 Hz from visual

observations of the data, and value from previous reports of humpback whales (Goldbogen et al. 2008; Ware et al. 2011; Simon et al. 2012) as a reference. Finally, IGOR Pro (binomial smoothing, 30 passes) was used to smooth the high-frequency acceleration data and remove noise at frequencies above the stroke rate that is likely to represent vibration of the suction cup and the tag. Pitch, roll and heading of the whales were calculated from the gravity-based acceleration and the tri-axial magnetism using 'ThreeD_path' macro compliant with IGOR Pro (Narazaki and Shomi 2010; Shiomi et al. 2010) where pitch angle is only used in this chapter.

2.2.4. Speed calibration

The swimming speed of an animal was calculated from the rotation counts of the propeller mounted on the accelerometer. Rotation counts were converted to speed with an equation obtained in a calibration experiment using an experimentally designed Blazka-type swim tunnel (Mori et al. 2015) with all five accelerometers (W1000-3MPD3GT). The accelerometers were set inside the tunnel and rotation counts were obtained under flow speeds ranging from 0.1 to 1.1 m s^{-1}, and the results were plotted as a regression line. All five accelerometers yielded high correlation coefficients (Range: 0.991 to 0.999; n = 10). Stall speed was also determined from the experiment to be 0.2 m s^{-1} for all loggers. Speeds below this value were considered indistinguishable from zero (Tanaka et al. 2001).

2.2.5. Dive and lunge events

The body diameter of humpback whales is reported to be 3.21 m (Woodward et al. 2006), so the start and end of each dive was defined as when the whale descended below and ascended above 4 m in depth, and it was extracted using the package Ethographer 2.00 in IGOR Pro (Sakamoto et al. 2009). Lunge events are characterized by a rapid acceleration in speed and energetic stroking (Ware et al. 2011; Simon et al. 2012). Using these characteristics, previous studies have identified lunge events from swimming speed obtained by flow noise (Goldbogen et al. 2006) or minimum specific acceleration and jerk (Simon et al. 2012). To explore the definition of lunges, lunge events were detected from video data and visually inspected the changes in acceleration and speed during lunges. Interestingly, even though there were variations in lunge speed, stroking effort was similar in all lunge events; therefore, the acceleration signal was used to extract the lunge events. A new method was used instead of jerk (estimated by differentiating the tri-axial acceleration signal which reveals fast movement or change in orientation of an animal; Simon et al. 2012), because it was simpler and could systematically detect the feeding event just as well. Following the method of Sakamoto et al. (2009), high-frequency strokes were identified by first generating a spectrum from acceleration signals of dorso-ventral axis. Then, each second of this spectrum was separated into four clusters by an unsupervised classification algorism, the *k*-mean clustering, and the two high-frequency clusters were considered the area of the lunge event. In some cases, however, high-frequency stroking was observed during the descent phase or at the surface. From visual observations in the field, as well as

from the attached video logger, the whales would first dive underwater and accelerate from below toward the surface, but no lunge event started from the surface or during the descent phase; therefore, high frequency stroking detected at depths shallower than 4 m or at negative pitch angles signifying the descent phase, was removed from the lunge counts. The accuracy of this method was verified using video data of two whales (WhB13 and WhB14), which showed 96.8% detection match of lunge events (331 dives with 129 lunge events during 10.2 hours of video data; two unmatched and two visually indistinguishable lunge events from video). A single lunge duration was defined as the beginning to the end of the high-frequency stroking phase plus five seconds, which was the approximate duration of the deceleration phase after the peak speed where mouth closing occurs (Simon et al. 2012; Cade et al. 2016). Patch residence time was defined as the beginning of the first lunge of a dive extending to the end of the last lunge of the same dive.

2.2.6. Video analysis

Identifying prey item and prey density

Video recordings were visually examined with VLC Media Player 2.0.2, and were synchronized with the accelerometer data from the surfacing phase of depth profile every 30 min. All videos recorded at 30 frames per second, were converted to still images of 640 × 480 pixels using Free Studio 6.4 (DVDVideoSoft Ltd., UK: Fig. 2-6A). At the same time pictures were sampled every one second. Due to low clarity of water in the bay the focal length of the camera was short and in

relation to swim speed of humpback whales (speed > 3 m s^{-1} during lunge), this sample rate of one second interval can generally avoid counting the same krill multiple times. These converted images were then imported to ImageJ software (Rasband 2012), within which all image analyses were conducted. Images were first converted to grey scale (8-bit) and filtered using the unsharp mask (radius 9.0, mask weight 0.7) and Gaussian blur (sigma 7) to make prey-like objects stand out from the background (Fig. 2-6B). The body of the whale and any other large objects, such as dolphins or other whales, were cleared out manually from all images and the remaining objects (prey) within the frame were marked using the command *Find maxima* (Fig. 2-6C). Finally, the number of objects and their area, the total area of the image, and the total area without large objects were calculated (in pixels) using the command *Analyze particle*. Using the values obtained, relative prey density, defined as the index of prey density (IPD) was first calculated every second by dividing the number of prey by the area without the body or any other large objects:

$$\text{Index of prey density (IPD)} = \frac{\text{Number of prey}}{\text{Area (in pixels) without large objects}} \quad [\text{unit}\cdot\text{pixels}^{-1}].$$

When the whales were at the surface or close to the surface, water bubbles at the surface were mistakenly detected as prey, generating unrealistically high values; therefore, measurements obtained from depths shallower than 4 m (same as the defined dive depth) were omitted.

Identifying other individuals

Video logger was also carefully observed to find any other factors that may influence the

whales' behavior, such as encounter with other animals that could be their competitor or predator. Dives were categorized as "present" or "absent" when other animals were seen or not seen, respectively, in the underwater footage. Animals observed at the surface, and the problem of animals being in a blind spot, due to the narrow view angle of the video, were disregarded in this study to avoid arbitrary judgments.

2.2.7. Foraging model

Here, a simple model is presented to test the efficiency of each dive based central place foraging theory (CPF) approach. Air-breathing marine predators, such as seabirds, marine turtles, and marine mammals, are considered "central place foragers," (Orians and Pearson 1979) due to their need to surface (central place) between foraging dives to breathe air (McNamara and Houston 1985; Tyson et al. 2016). The central place foraging theory (CPF) is the most effective model under optimal foraging theory which developed to predict how a central place foragers maximizes the energy intake per unit time (currency) in relation to change in prey density under constraints: (1) the time cost of moving back and forth between patches and water surface; and (2) the post-surface time where they restore oxygen, because of the trade-off between energy intake and oxygen depletion associated with dives (Orians and Pearson 1979; McNamara and Houston 1985; Hazen et al. 2015). Longer dives consume more oxygen, resulting in a longer post-surface recovery time (Kooyman and Ponganis 1998; Goldbogen et al. 2008).

In this study, foraging humpback whales are assumed to encounter a single patch of prey per dive. Foraging cycle of humpback whales in a single dive include, 1) a transit/dive phase to the underwater prey patch, 2) patch residence time, where actual lunge feeding phases with acceleration to high speed, engulfment of water and prey, and the filtration of water (Potvin et al. 2010; Cade et al. 2016) occur once to several times, and finally 3) transit to the surface, and post-surface phase where they restore oxygen (Fig. 2-7A), a factor essential for a model of air-breathing divers (Stephens et al. 2007). Therefore, the energy gain per unit time over a single dive is the currency optimized by humpback whales and the travel time, post-surface recovery time, and change in rate of energy intake in relation to change in prey density over time is the constraints. Search dives are distinguishable between foraging dives which are often seen before humpback whales start its continuous feeding dives, therefore; is not included in this model.

Rate of energy intake (*Ec*)

A gain function was constructed by calculating the energy intake of each lunge from IPD, where each lunge event is indicated by a red line in Fig. 2-7A. Here the density of prey (prey in each frame) passing by the humpback whales are assumed to be proportional to the energy intake of filter-feeders, therefore; the sum of IPD during each lunge event was regarded as the relative energy intake of each lunge event. Cumulative of this relative energy intake (unit·pixels^{-1}; termed cumulative energy intake, hereafter) during each lunge was plotted as a linear function (black line on

the right-hand side of Fig. 2-7B), with each point corresponding to the time and the cumulative energy intake after each lunge in that particular foraging dive. The slope inclination from the beginning of patch residence time to the end of the first lunge corresponded to the rate of energy intake of the first lunge (*Ec*: unit·pixels^{-1}·sec^{-1}). From the second lunges, the slope inclination between two lunges corresponded to the rate of energy intake (*Ec*: unit·pixels^{-1}·sec^{-1}) during the period from end of preceding lunge until the end of the subsequent lunge. This gain function was constructed for all dives with at least two lunges per dive.

Total rate of energy intake (*En*)

The total rate of energy intake per unit time during a single dive cycle (*En*) was calculated from the cumulative energy intake over the duration of each foraging cycle. The left-hand side of the horizontal axis of Fig. 2-7B indicates the transit duration (descent + ascent) and the post-surface duration, which are the areas indicated in pink in Fig 2-7A. The slope of the blue line in Fig. 2-7B, starting from the sum of the transit duration and the post-surface duration to the lunge point on the right-hand side, indicates the total rate of energy intake (*En*) after the last lunge:

$$\text{Total rate of energy intake } (En) = \frac{\text{Sum of cumulative energy intake of lunges}}{\text{Duration (Transit + Post-surface + Patch)}} \ [\text{unit} \cdot \text{pixels}^{-1} \cdot \text{sec.}^{-1}]$$

This total rate of energy intake (*En*) was calculated for all lunge points in a dive.

Investigating the efficiency

The concept of the CPF was applied to interpret the time efficiency of a foraging event up to every lunge of a dive, by comparing the rate of energy intake (*Ec*) with the total rate of energy intake (*En*) after each lunge, for dives with greater than or equal to two lunge events. According to CPF humpback whales will leave the prey patch when the total rate of energy intake (*En*) in a single dive cycle is maximized. The *En* in a single dive cycle is maximized when it overlaps with the rate of energy intake (*Ec*) (Fig. 2-7B).

2.2.8. Statistics

All statistical analyses were performed with R2.15.2. (R Core team 2015). There are two types of air-breathing divers. One is the anticipatory breathing divers, which anticipate the length of dives and accordingly load the oxygen needed for the subsequent dive. These animals show stronger correlation between pre-surface duration and dive duration. Another is the reactive breathing divers, which replenish oxygen store after each dive. These animals show stronger correlation between post-surface duration and dive duration (Lea et al. 1996; Mori et al. 2002) Humpback whales are known to be reactive breathing divers, although; in order to confirm that post-surface duration is more associated to foraging dive duration than pre-surface duration, a generalized linear model (GLM) with gamma distribution was used. The response variable was foraging dive duration and the explanatory variables were pre-surface duration or post-surface duration. The Akaike Information

Criteria (AIC) were compared between the two combination and the result with the smaller value was considered as the most parsimonious model. Correlations between patch residence time and the number of lunges per dive, as well as correlations between post-surface duration and dive duration were calculated as Spearman's rank correlation coefficients. Statistical significance was set at $P < 0.05$. The difference between the two slopes (i.e. the rate of energy intake and the net rate of energy intake), was compared using the Mann–Whitney *U* test (Wilcoxon rank test). Statistical significance was set at $P < 0.05$. Liner regression model was also used to assess the relationship between *Ec* and *En* of each lunge number in order to visually observe the efficiency of each lunge event in a dive. According to the CPF, animals are expected to stop feeding when *En* is maximized. This is when *Ec* = *En* (*Ec*/*En* = 1). When the value of *Ec*/*En* > 1, *Ec* is still greater than *En*, thus the whales are expected to continue feeding. When *Ec*/*En* < 1, this implies that *Ec* has dropped below the point which maximum rate of energy intake can no longer be obtained in that dive cycle, thus the whales are expected to stop feeding. *Ec* of single lunge dives and *Ec* of the first lunge of multiple lunge dives were also compared using Man-Whitney *U* test. Statistical significance was set at $P < 0.05$.

A statistical model was constructed to examine whether the presence/absence of other individuals influenced the patch residence time. The response variables were number of lunges per dive (*M*) and patch residence time (*T*); the explanatory variables were presence/absence of other individuals (*O*), dive depth (*D*), and maximum IPD (*MIPD*), and individual variations were set as the random effect. The lunge number was modeled using Poisson distribution,

$$M \sim Poissson(\lambda)$$

where λ is a mean value represented as,

$$\lambda = \exp(a + a_O O + a_D D + a_{MIPD} MIPD + r_{M,i})$$

where a_O, a_D and a_{MIPD} are coefficients of presence/absence of other individuals (O), depth (D) and maximum IPD ($MIPD$), respectively. O takes 0 when other individuals were absent and 1 when other individuals were present. The $r_{M,i}$ represents random effect of individuals on number of lunges per dive, where i represents the index of individuals. The patch residence time was modeled using Gamma distribution as

$$T \sim Gamma(\alpha, \alpha / \mu)$$

where α is the shape parameter and μ is the mean value modeled as

$$\mu = M \exp(b + b_O O + b_D D + b_{MIPD} MIPD + r_{T,i}) + (M - 1) q \ .$$

The b_O, b_D and b_{MIPD} are coefficients and $r_{\mathrm{T,i}}$ is the random effects of individual variation on duration per lunge. $\exp(b + b_O O + b_D D + b_{MIPD} MIPD + r_{T,i})$ corresponds to the duration per lunge (Fig. 2-7A; each red line). q represents the time interval between successive lunges. When there are M lunges in a dive, (M-1) intervals are included (For example, there are 3 intervals in 4 lunges dives as in Fig. 2-7A). Hence, total patch residence time in a dive is modeled as above. $r_{T,i}$ and $r_{M,i}$ were assumed to be normally distributed.

$$r_{T,i} \sim Normal(0, \sigma_T), r_{M,i} \sim Normal(0, \sigma_M).$$

The prior distribution of σ_T and σ_M were set to be normal distributions whose means are 0 and

standard deviations are 10. By conducting MCMC, posterior distributions and 95% confidence intervals (95% CI) for each parameter were computed. For MCMC sampling, the RStan library (rstan) was used. Among the parameters, the 95% CI of presence and absence of other animals (a_O, b_O), depth (a_D, b_D), and maximum IPD (a_{MIPD}, b_{MIPD}), were of special interest in this study.

2.3. Results

2.3.1. Foraging characteristics

Seven humpback whales were tagged in Skjálfandi Bay off Húsavík in northern Iceland. A total of 82 hours of behavioral data were obtained from these whales, as well as 45 hours of video data from six of them (Table 2-1). All tagging was conducted and retrieved within the bay.

There were a total of 2860 dives during the 82 hours. The mean surface duration, dive duration, and dive depth of 2860 dives were 52.7 ± 36.6 sec, 85 ± 34.9 sec, and 27.8 ± 10.8 m (± s.d.), respectively (Table 2-1). Among the 2860 dives, 1914 of them were feeding dives. The number of lunges counted in each feeding dive varied among dives (Fig. 2-8A), ranging from one to maximum of seven with a median of two, and there was a positive correlation between patch residence time and the number of lunges per dive (Spearman's $\rho = 0.92$, $P < 0.001$; Fig. 2-8B). The feeding dive depths of each whale ranged from 4 to 97 m with a mean diving depth range being 16 to 35 m.

At this study site, humpback whales did not feed cooperatively with bubble net feeding;

rather, they fed individually identified from visual observation in the field and video logger attached to whales. Peaks of simultaneous body acceleration indicating lunge events were identified during the ascent phase of dives (Fig. 2-8A) and maximum pitch angle of the body during this phase was 44.1 ± 27 degrees (± s.d., n = 2684), where 0 degrees is when humpback whales are completely horizontal to the surface and positive 90 degrees will be when the head is vertically up to the surface and negative 90 degrees will be when head is vertically down. This suggests that humpback whales of Iceland feed by vertical lunge feeding.

Krill was the only prey observed with the video-logger and relative density of prey in front of each whale was estimated from the video recordings throughout the dives (Fig. 2-9). However, only data from dives shallower than 35 m were used for analysis involving prey density, as the images became too dark to make estimates at greater depths. Highest frequency of lunge occurred around 16 to 24 m and the peak of highest krill density was observed around 19 m to 20 m (Fig. 2-10).

2.3.2. Foraging efficiency when alone

The post-surface duration was more associated to foraging dive duration of humpback whales as first predicted. The AIC values for pre-surface model and post-surface model was, 19489.40 and 19232.19, respectively (n = 1991). The AIC value of post-surface duration was smaller thus, post-surface duration was used for constructing the foraging model. All the feeding dives of two whales (ID: WhA14, WhD14) exceeded 35 m, therefore; the analysis to investigate the efficiency of

a single foraging dive was restricted to four whales (ID: WhB13, WhB14, WhC14, WhE14; Table 2-1). Four whales performed 578 dives in total, including 251 dives with lunge events. Even though the depth was shallower than 35m and the range of lunge number counted in each foraging dive was now one to four with a median of one, there was still a positive correlation between patch residence time and the number of lunges per dive (Spearman's $\rho = 0.78$, $P < 0.001$; Fig. 2-11).

There were 70 feeding dives with at least two lunges, within the 251 feeding dives. To verify the consistency of the data with previous reports which show positive relationship between dive duration and post-surface duration, the relationship between the two variables were confirmed again for these 70 feeding dives. This showed a positive relationship between post-surface duration and dive duration (Spearman's $\rho = 0.54$, $P < 0.0001$; Fig. 2-12), which agreed with the previous studies (Friedlaender et al. 2016b). Then, gain function of the foraging model was calculated for these 70 dives and 90% showed a gradual decrease over lunges (Fig. 2-13B). The model for dives with two lunges indicated higher rates of energy intake (*Ec*) in comparison with the total rate of energy intake (*En*) during the first lunge (Mann–Whitney *U* test, $P < 0.01$, $n = 49$; blue and red lines did not overlap in Fig. 2-14A) having *Ec*/*En* equaled to 4.1 (95% CI: 3.8 – 4.3; Table 2-2: Fig. 2-14C). However, during the last lunge in the CPF model, the rates of energy intake (*Ec*) overlapped with the total rate of energy intake with no significant difference (*En:* Mann–Whitney *U* test, $P = 0.30$, $n = 49$; Fig. 2-14B), and *Ec*/*En* was equaled to 0.88 (95% CI: 0.79 – 0.98; Table 2-2: Fig. 2-14D). Statistically, this value is less than one, yet is a value very close to one. Dives with three lunges had

higher *Ec* in comparison with *En* during the first (Mann–Whitney *U* test, $P < 0.01$, $n = 17$; Fig. 2-14E) and second lunges (Mann–Whitney *U* test, $P < 0.05$, $n = 17$; Fig. 2-14F); *Ec*/*En* of 5.1 (95% CI: 4.5 – 5.7) and 1.5 (95% CI: 1.2 – 1.8, Table 2-2), respectively (Fig. 2-14HI). However, during the last lunge, again, *Ec* overlapped with *En* ((Mann–Whitney *U* test, $P = 0.39$, $n = 17$; Fig. 2-14G), having *Ec*/*En* equaled to 1.2 (95% CI: 0.99 – 1.3; Table 2-2: Fig. 2-14J). Overall, the value of *Ec*/*En* of the three-lunge dive was greater than the *Ec*/*En* of the two-lunge dive. Statistical analysis could not be conducted for the case of dives with four lunges due to small sample sizes ($n = 2$); however, the dive had a similar trend with other dives (Fig. 2-14K-N), with *Ec* and *En* overlapping on the last lunge (Fig. 2-14N). Because foraging model could not be used to assess the single lunge dives ($n = 155$), we simply compared the *Ec* of the single lunge dives with *Ec* of the first lunge of multiple lunge dives. This showed a significant difference with higher *Ec* for multiple lunge dives (Mann-Whitney *U* test, $P < 0.0001$; Fig. 2-15).

2.3.3. Effect of other individuals

Other humpback whales and white-beaked dolphins (*Lagenorhynchus albirostris*) were sometimes seen in video data of two of the tagged whales (ID: WhB14 and WhC14), but no predator-like animals such as killer whales (*Orcinus orca*) or sharks were spotted, this eliminating the risk of predation on the whales for this study. Since dolphins do not feed on krill and is not a direct competitor they were disregarded in this study. Other humpback whales were seen in 16 dives

from two whales (Fig. 2-16; ID: WhB14 and WhC14) and 12 out of those 16 dives were feeding dives. The maximum number of lunges in dives with no other animal was four, whereas it was two in present dives which only occurred once, and all other foraging dives were single lunge dives.

Patch residence time in a single dive was shorter when humpback whales encountered other humpback whales (Fig. 2-17). The negative value of a_O and b_O (Table 2-3) indicates that the presence of other individuals decreases the lunge number, and the duration per lunge. Based on the 95% CI of a_O and b_O, the effect of presence/absence of other individuals was significant for duration per lunge (b_O), but not for number of lunges per dive (a_O) as 95% CI are not completely negative. The values of a_D, b_D, a_{MIPD} and b_{MIPD} were all positive (Table 2-3). This indicates that the lunge number and duration per lunge increases as depth and maximum IPD increases; as a result, increase in patch residence time (Fig. 2-17). These effects were all significant except for MIPD on number of lunges (a_{MIPD}) as 95% CI were not completely positive for a_{MIPD}. (Table 2-3).

2.4. Discussion

2.4.1. Foraging characteristics

Humpback whales are believed to be selecting the most suitable and efficient way for capturing preys (Weinrich et al. 2009; Acevedo et al. 2011). For instance, bubble net feeding is often seen among population that are in groups feeding on small schooling fish. Lateral lunge feeding is also reported among the community that feed on small fish. Vertical lunge feeding, on the other hand is

seen among the ones that feed individually on less agile prey such as krill. This study indicated that humpback whales in Skjálfandi Bay feed individually using vertical lunge feeding. Moreover, they were mainly feeding on krill. This prey type and lunge feeding type both agrees with the previous reports (Acevedo et al. 2011).

Humpback whales are often reported feeding over 100 m in depth (Goldbogen et al. 2011; Ware et al. 2011; Simon et al. 2012). The bathymetric depth of the Skjálfandi bay can go up to 250 m, although the maximum feeding depth observed was 97 m and they generally fed at shallow depth of 25.1 ± 7.0 m in average. In the case of humpback whales, it has been predicted that if prey density is constant over depth, foraging efficiency should increase with decreasing depth, because overall feeding rate could be increased at shallower depth (Ware et al. 2011). The humpback whales in Skjálfandi Bay may be efficiently feeding by behaving in a way as this prediction, with shallow and mostly single lunge per dive. Moreover, estimation of relative prey density indicated that humpback whales were frequency feeding at depth which was abundant in prey (Fig. 2-10). Although, previous studies predicted that the optimal foraging depth for animals is always shallower than the depth of highest prey density (Mori 1998) and humpback whales were observed feeding at the upper boundary of the patch rather than diving deeper to higher density area (Goldbogen 2008). Assuming from their shallow foraging depth there is a possibility that humpback whales in Iceland was also behaving in this way, but from this study this phenomenon could not be identified. Regardless, this study indicated that their feeding depth is associated with prey depth and prey was abundant at the

shallow depth that they were feeding at. Thus, there is no need for the humpback whales to waste energy for unnecessary deep dives to feed. These feeding characteristics suggests that humpback whales in this bay are making choice of the most energetically efficient way and depth for them to capture prey.

2.4.2. Foraging efficiency when alone

Assessing the predator–prey interactions of free-ranging diving marine predators is challenging. When studying the predator–prey interactions of rorquals, ship-mounted echo-sounders were commonly used to measure the distribution and abundance of prey near tagged whales in previous studies (Goldbogen et al. 2008; Hazen et al. 2009; Nowacek et al. 2011; Goldbogen et al. 2015; Hazen et al. 2015; Friedlaender et al. 2016a; Friedlaender et al. 2016b). The advantage of this method is that it maps the prey distribution in the feeding grounds of whales at wider and deeper ranges over a long period of time. Recent study of humpback whales using a ship-mounted echo-sounder revealed that the foraging decisions of humpback whales are driven by both prey depth and density. Humpback whales maximized the energy intake over time by mainly feeding at a shallow depth to minimize their diving and search cost and to increase overall feeding rate (Friedlaender et al. 2016b).

The disadvantage of the previous method was that it could not reveal the temporal changes in prey density during each feeding event; therefore, momentary information on the prey density

encountered by whales in the time and places where feeding occurred was not obtained. The new method used in present study filled this gap and assessed the relative prey density from the video loggers attached to the whales, providing information on the temporal changes in prey density in front of the whale and linked it to their behavior.

This study indicated a statistically significant positive relationship between patch residence time (number of lunges per dive) and depth, which agreed with the previous report by Friedlaender et al. (2016b). Patch residence time also increased with maximum IPD, although this was not statistically significant (Table 2-3). This may be because this analysis was restricted to shallow depth, and krill patch density within 35 m was fairly constant. Yet, this method succeeded to test the decision making of humpback whale based on CPF (i.e. the energy intake rate maximization strategy within a single dive cycle). The rate of energy intake (*Ec*) during each lunge showed a gradual decrease through consecutive lunge events in the majority (90%) of dives (diminishing return). This may be an indication of decrease in prey density due to large amount of prey consumed during each lunge event, or prey being dispersed from passing through the aggregated patch of prey on the previous lunge. Under the condition of diminishing return, humpback whales stopped feeding when the slopes of total rate of energy intake (*En*) and rate of energy intake (*Ec*) overlapped on the model (*Ec*/*En* was very close to one or less). Moreover, rate of energy intake of single lunge dives was significantly lower than the rate of energy intake of the first lunges of multiple-lunge dives (Fig.2-15). This implies that humpback whales were efficiently feeding by adjusting their foraging duration or

number of lunges per dive in relation to decreasing prey density so that the rate of energy intake in a single dive cycle is nearly maximized. Some studies of optimal foraging for air-breathing divers considered the physiological constraint of oxygen store as the dominant factor affecting the decision making of air-breathing divers (Houston and Carbone 1992; Thompson and Fedak 2001; Doniol-Valcroze et al. 2011). In these studies, energy intake was assumed to be linear (i.e. no diminishing return, however, see Mori et al. 2002; Mori and Boye 2004) and the foraging duration to be strongly constrained by the diminishing cumulative oxygen uptake (Foo et al. 2016). In this study, however, the gain function diminished drastically, and foraging duration was expected to be more constrained by diminishing rate of energy intake (ecological constraint) than the oxygen store (physiological constraint), therefore; did not consider the oxygen store as a dominant constraint for simplicity of this study.

2.4.3. Effect of other individuals

The video-based method provided an unexpected opportunity to assess predator–prey–competitor interactions in humpback whales. Analyses showed a decrease in patch residence time in the presence of other humpback whales (Fig. 2-17). This suggests that not only depth and prey density, but also the presence/absence of other animals affects the foraging behavior of humpback whales. Other humpback whales in this field are recognized as direct competitors feeding on the same patch of krill. Humpback whales fed until the total rate of energy intake (*En*) in a single dive

cycle was nearly maximized when alone (Fig. 2-17). In comparison, when other humpback whales were present, the patch residence time was shorter, and most dives only contained one lunge event. Thus, in presence of competitors, humpback whales might have left the patch or ended the dive early because patch quality was already decreased by the foraging activity of other individuals or considering the potential decrease in prey abundance due to competition (Fig. 2-18). Although sample size of dives with other individuals was rather small in this study, the results show an interesting trend and introduce a new potential to quantitatively investigate the effect of other individuals on feeding top predators in natural condition.

Table 2-1. Tagging results of seven humpback whales. The table shows whale ID, tagging date, and number of hours of accelerometer and video data obtained. Asterisks (*) indicate data used in the analyses. The general dive characteristics (feeding and non-feeding dives) of each whale are presented as mean value ± s.d.

ID	Date of attachment	Accelerometer (h)	Video (h)	Number of dives	Surface duration (sec.)	Dive duration (sec.)	Dive depth (m)
WhA13	5 Jun. 2013	4.1	N.A.	218	15.9 ± 13.2	53.0 ± 39.4	19.3 ± 4.5
WhB13*	7 Jun. 2013	24.5	2.9	1315	28.5 ± 60.2	39.6 ± 46.8	17.0 ± 7.6
WhA14	25 Jun. 2014	12.5	11.5	216	125.0 ± 324.8	81.4 ± 109.6	21.5 ± 23.4
WhB14*	27 Jun. 2014	13.1	7.3	412	41.5 ± 114.6	73.6 ± 52.0	23.1 ± 10.1
WhC14*	28 Jun. 2014	17.2	12.5	493	30.9 ± 40.6	92.8 ± 100.4	29.9 ± 21.8
WhD14	29 Jun. 2014	6.6	6.6	132	67.6 ± 202.1	111.3 ± 66.0	36.7 ± 17.8
WhE14*	29 Jun. 2014	4.2	4.2	74	59.6 ± 53.8	143.0 ± 71.1	47.1 ± 17.5

Table 2-2. Values of Ec/En and 95% CI for each lunge in a dive.

	Ec / En	95% CI
First lunge of two-lunge dive	4.1	3.8 – 4.3
Second lunge of two-lunge dive	0.88	0.79 – 0.98
First lunge of three-lunge dive	5.1	4.5 – 5.7
Second lunge of three-lunge dive	1.5	1.2 – 1.8
Third lunge of three-lunge dive	1.2	0.99 – 1.3

Table 2-3. 95% CI for each parameter based on prior distributions computed by MCMC sampling. The parameters indicate positive relationship when the mean is positive and negative relationship when the mean is negative. The data are statistically significant when 95% CI is either completely positive or completely negative.

Coefficients (explanatory variable, unit)	**Mean**	**95% confidence intervals**		
a_D (depth, m)	0.18	0.11	-	0.23
a_{MIDP} (MIDP, unit·pixels^{-1})	0.31	- 0.19	-	0.71
a_O (others, unit)	-1.1	-4.3	-	0.63
b_D (depth, m)	0.0068	0.0016	-	0.011
b_{MIDP} (MIDP, unit·pixels^{-1})	0.068	0.011	-	0.11
b_O (others, unit)	-0.12	-0.21	-	-0.031

A

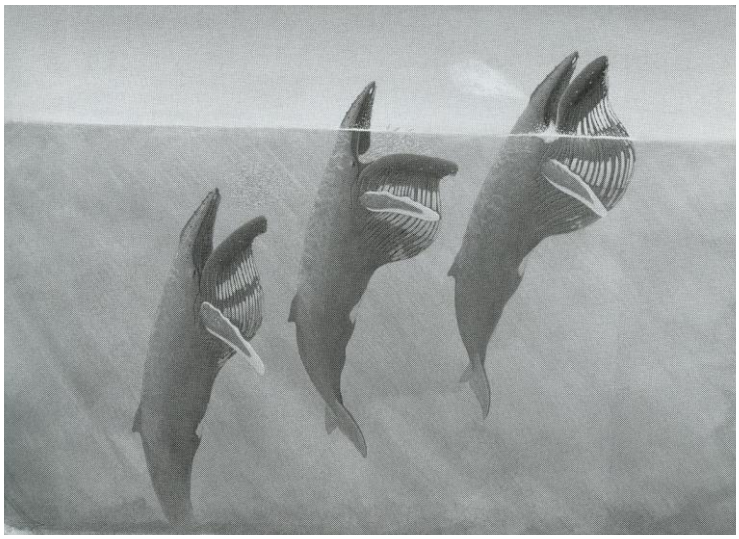

B

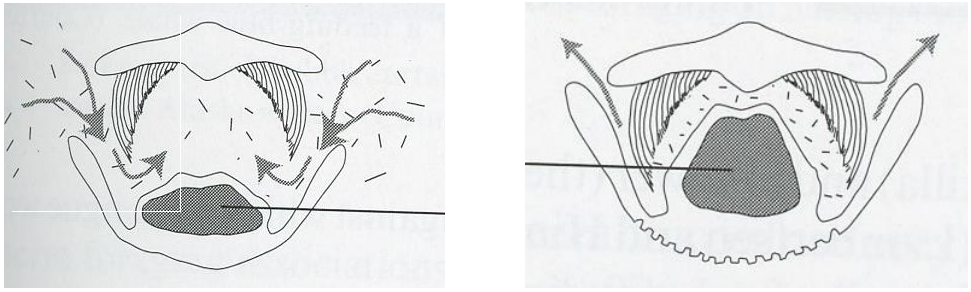

Figure 2-1. Mechanics of lunge feeding. (A) Lunge feeding process of humpback whale. (B) Water being pushed out, trapping the prey inside its mouth (Figures extracted from Berta 2005).

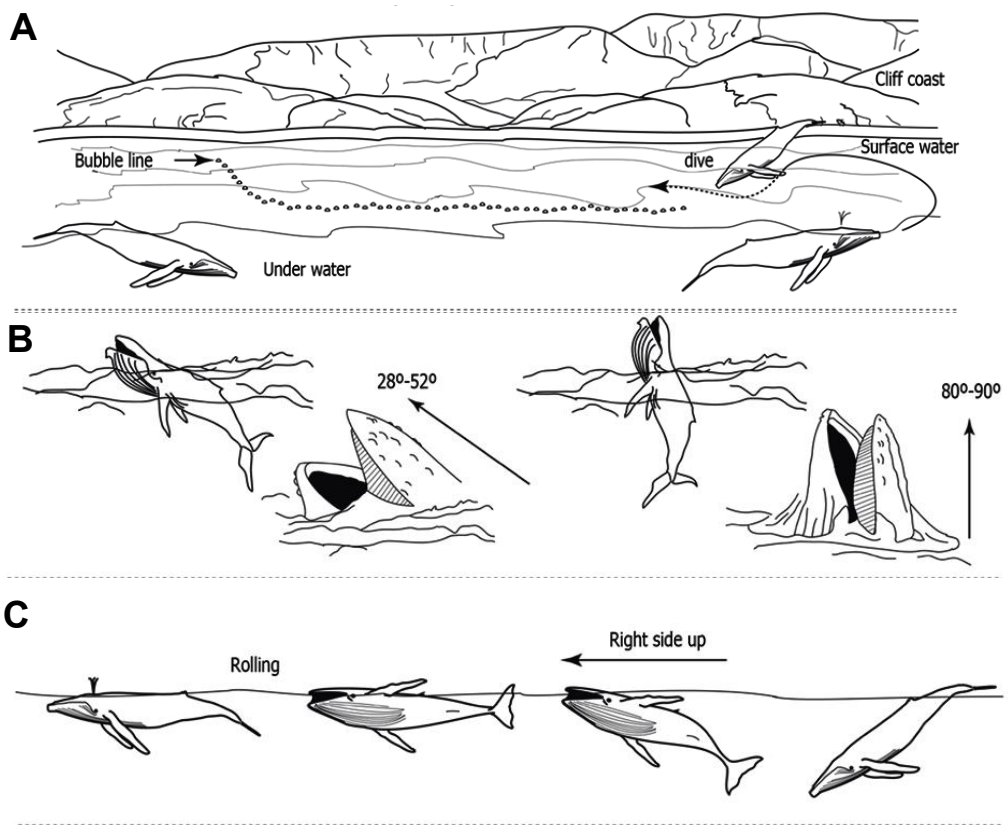

Figure 2-2. Diagram of (A) bubble-cloud (net) feeding, where humpback whales first produces a net of bubble to clump the prey into a tight food ball and then lunge into the food ball. (B) vertical lunge feeding, (C) lateral lunge feeding (Figures extracted from Acevedo et al. 2011).

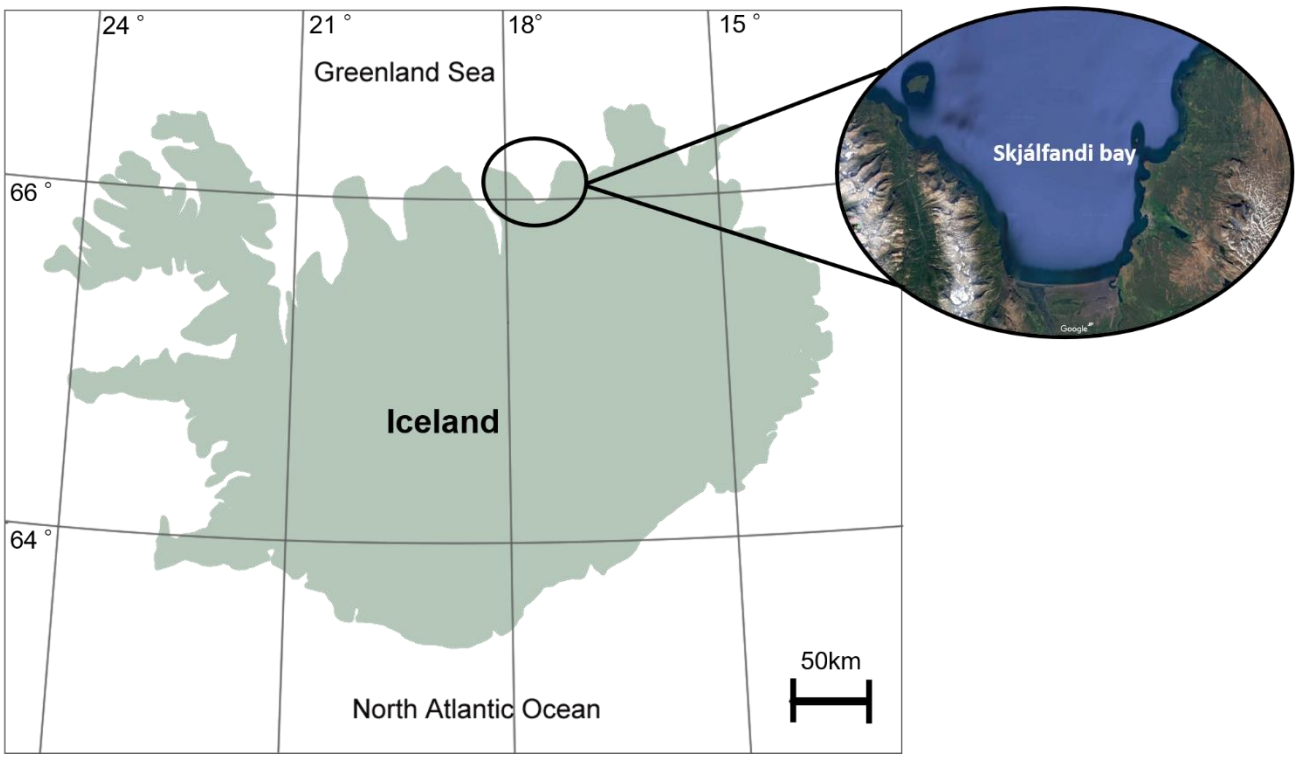

Figure 2-3 Study site in Iceland and Skjálfandi Bay.

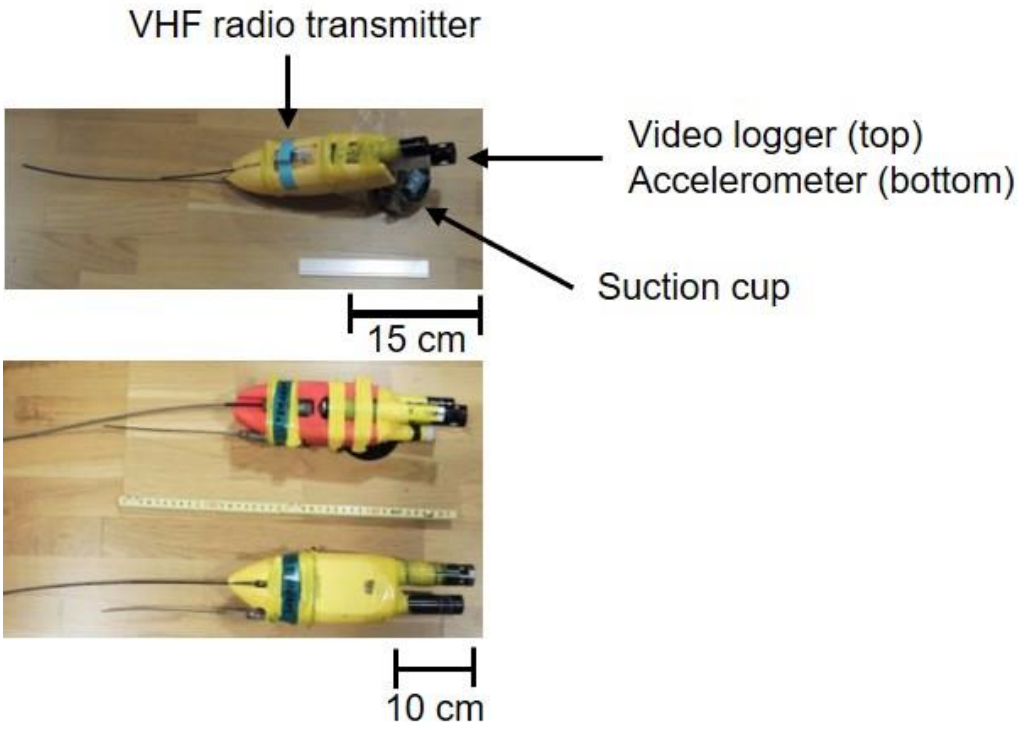

Figure 2-4. Tag with accelerometer, video logger, VHF radio transmitter and a suction cup. Top figure is the model used in 2013 and bottom is the model used in 2014.

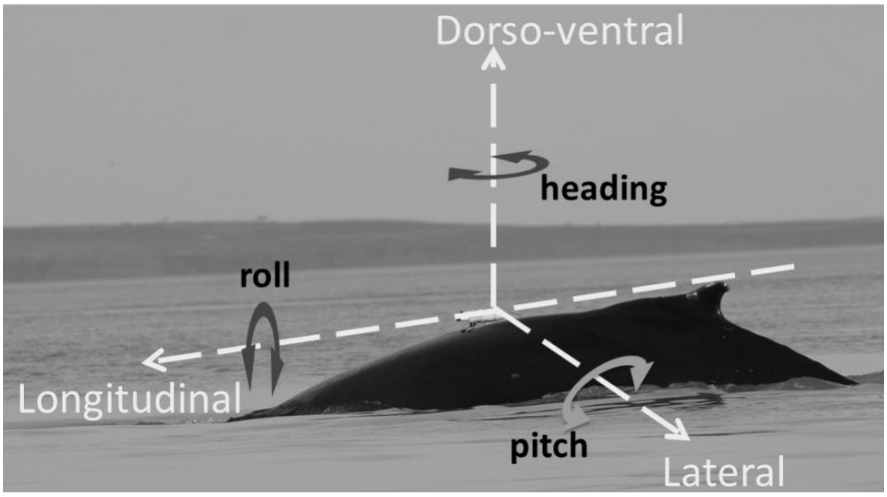

Figure 2-5. Orientation from 3 axis acceleration and 3-axes magnetism of accelerometer.

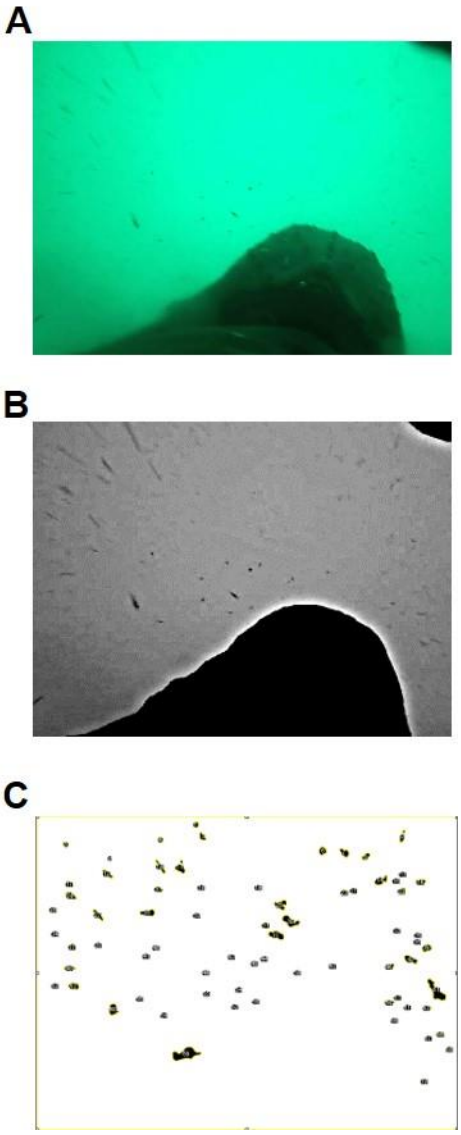

Figure 2-6. Example of video analysis for counting prey. (A) Video data converted to still image (B) Images converted to grey scale and filtered (C) Image with the body of the whale and large objects removed and the remaining objects (prey) being marked.

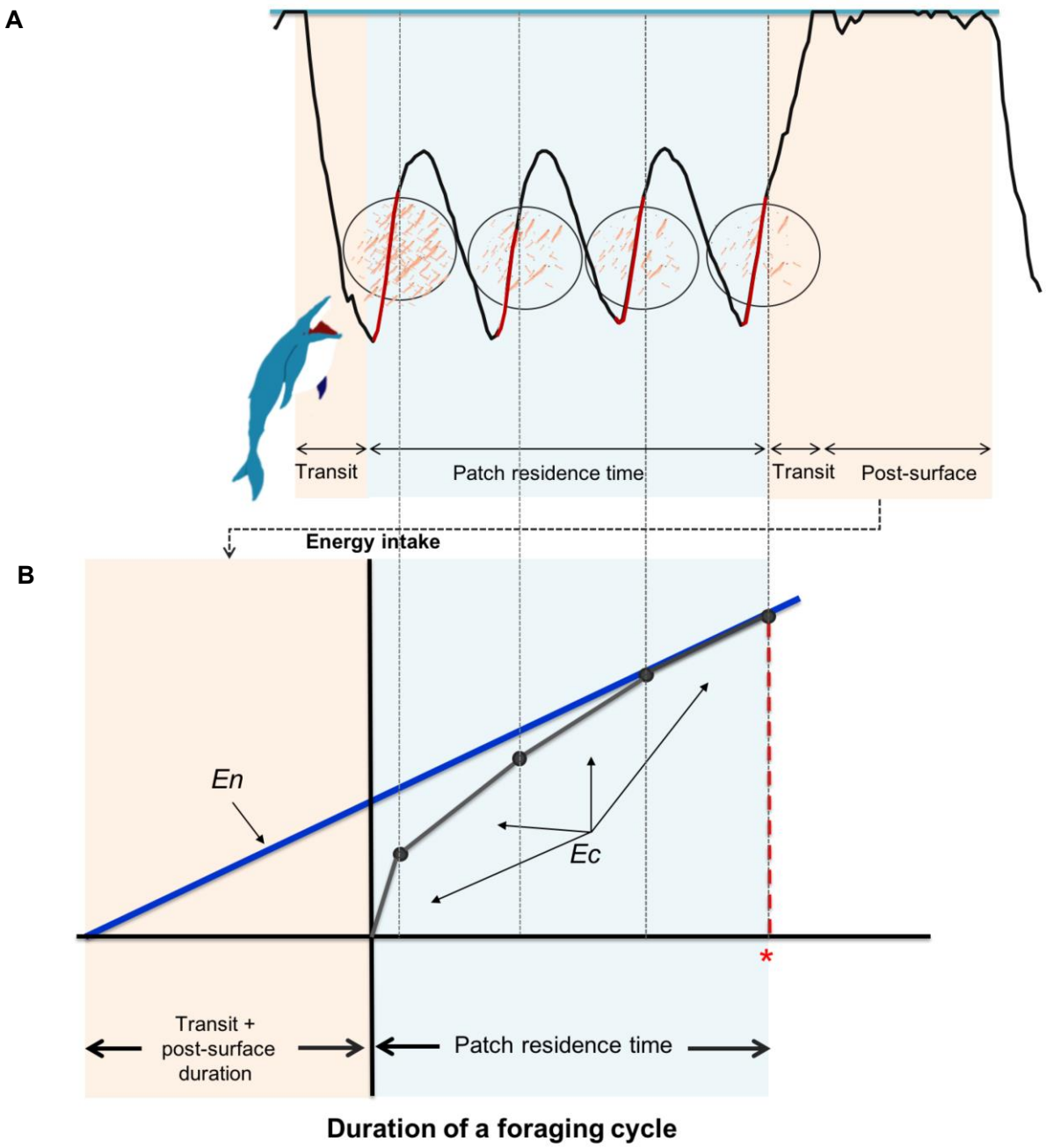

Figure 2-7. Illustration and diagram showing a gain function of a single dive with the optimal patch time according to the assumption of CPF. (A) A depth profile of a whale lunging (red lines) four times in a single dive. The energy intake of each lunge is the sum of the Index of Prey Density measured over the lunge duration (red line). (B) Rate of energy intake is plotted as a slope of linear functions (*Ec*; black line on the right-hand side), with each black dot representing the duration and

cumulative energy intake at each lunge. Here, the prey density is predicted to decrease after each lunge showing a shape of a diminishing rate of energy intake (slope of a line). The left-hand side shaded in pink indicates the transit duration (descent + ascent) and the post-surface duration. The slope of the blue line starting from the sum of the transit and surface duration to the last lunge point on the right-hand side indicates the total rate of energy intake (*En*) of this whole foraging cycle. The optimal patch time is indicated in red *, which in this case is where *Ec* and *En* overlaps.

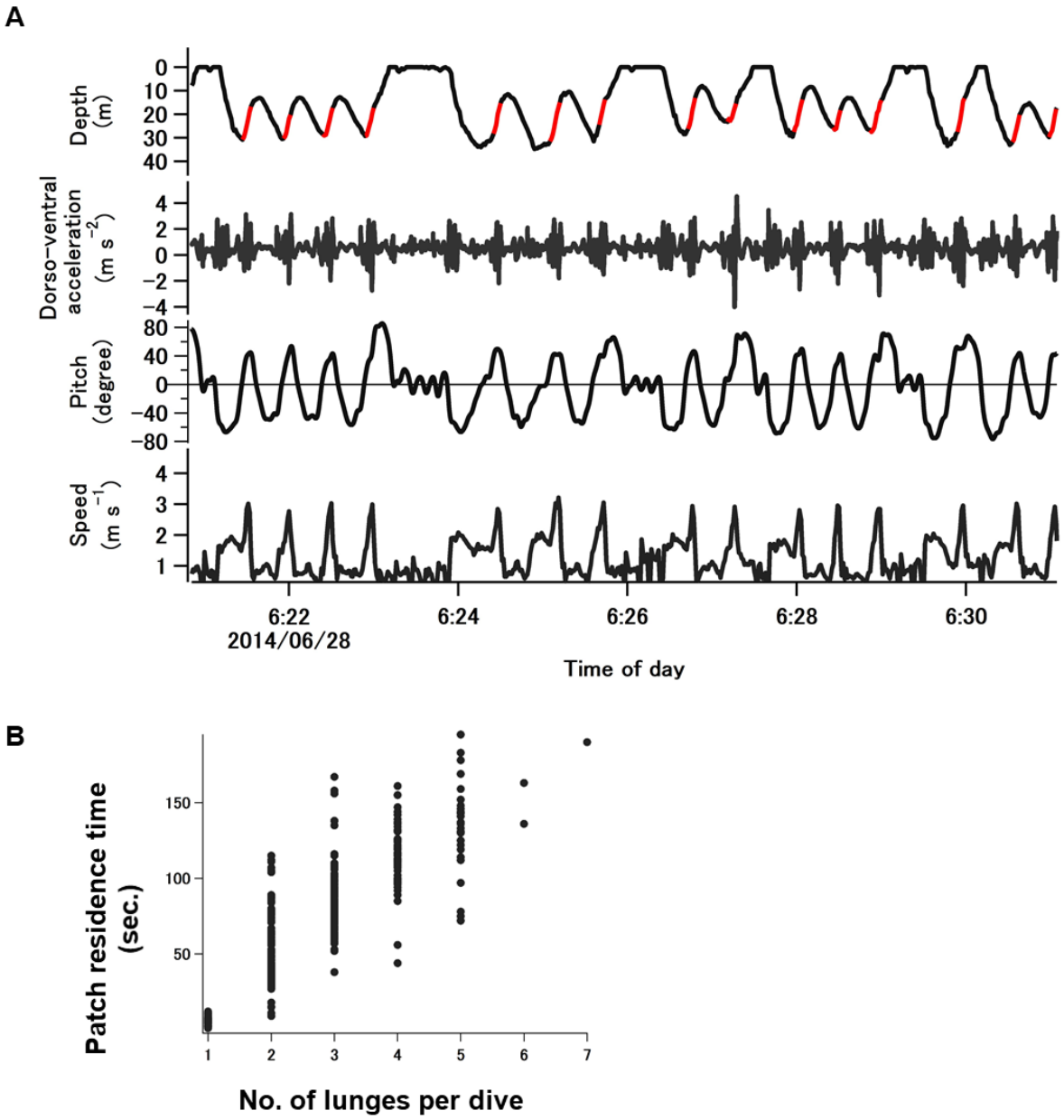

Figure 2-8. Characteristics of lunge dives. (A) Diving behavior of a humpback whale (ID: WhC14). Dive profile with lunge events (indicated in red), dorso-ventral acceleration, pitch angle and swim speed in dives with varying numbers of lunges per dive (B) Relationship between patch residence time and number of lunges per dive, showing positive correlation (Spearman's $\rho = 0.92$, $P < 0.001$).

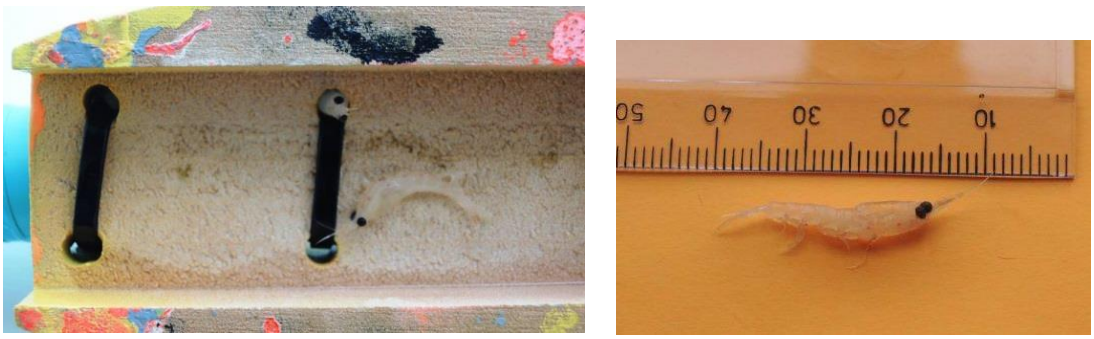

Figure 2-9. Krill found inside the retrieved tag.

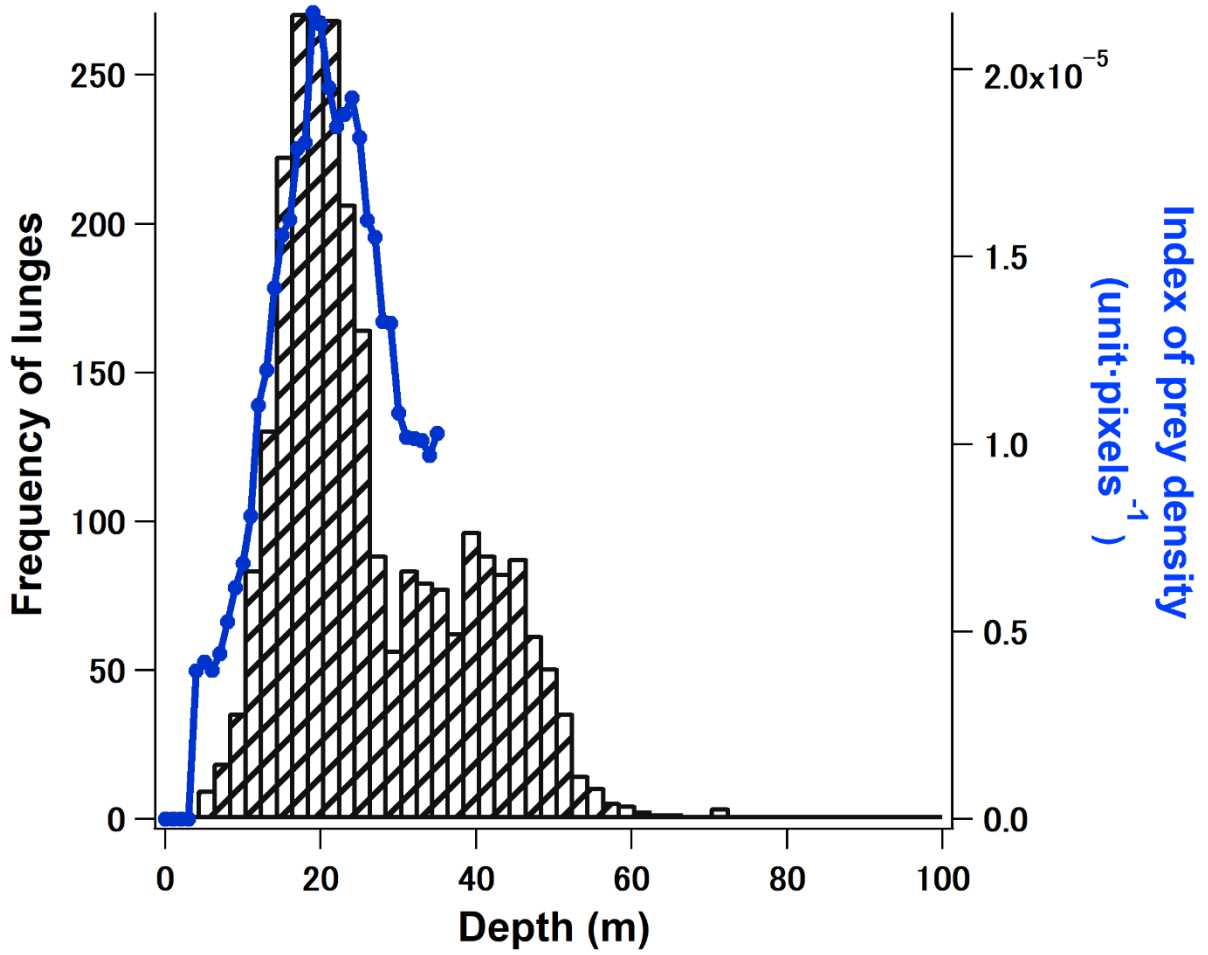

Figure 2-10. Histogram showing the frequency of number of lunge event and line indicating mean Index of prey density at each depth (Mean IPD = $\frac{\sum_{i=1}^{n} IPDi}{n}$, where n is the number of lunges at that certain depth). The lunge depth in this figure is the mid-point depth of the acceleration phase (Fig. 2-7A, red line).

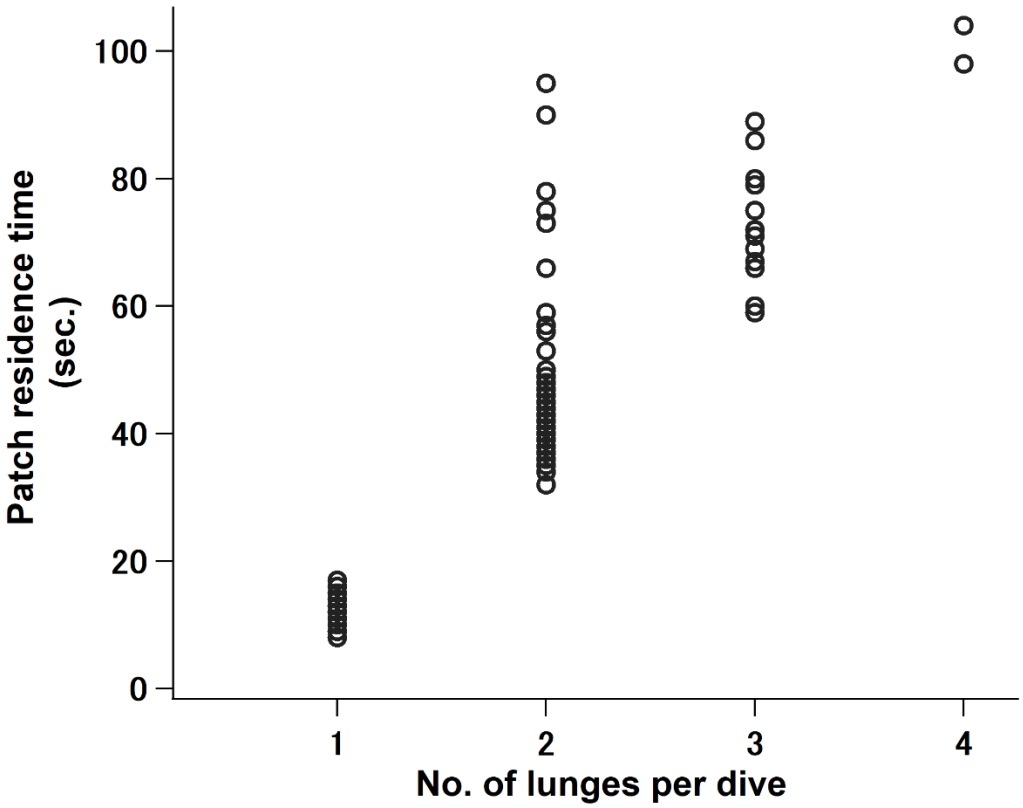

Figure 2-11. Relationship between patch residence time and number of lunges per dive within lunge dives shallower than 35m, showing positive correlation (Spearman's $\rho = 0.78$, $P < 0.001$).

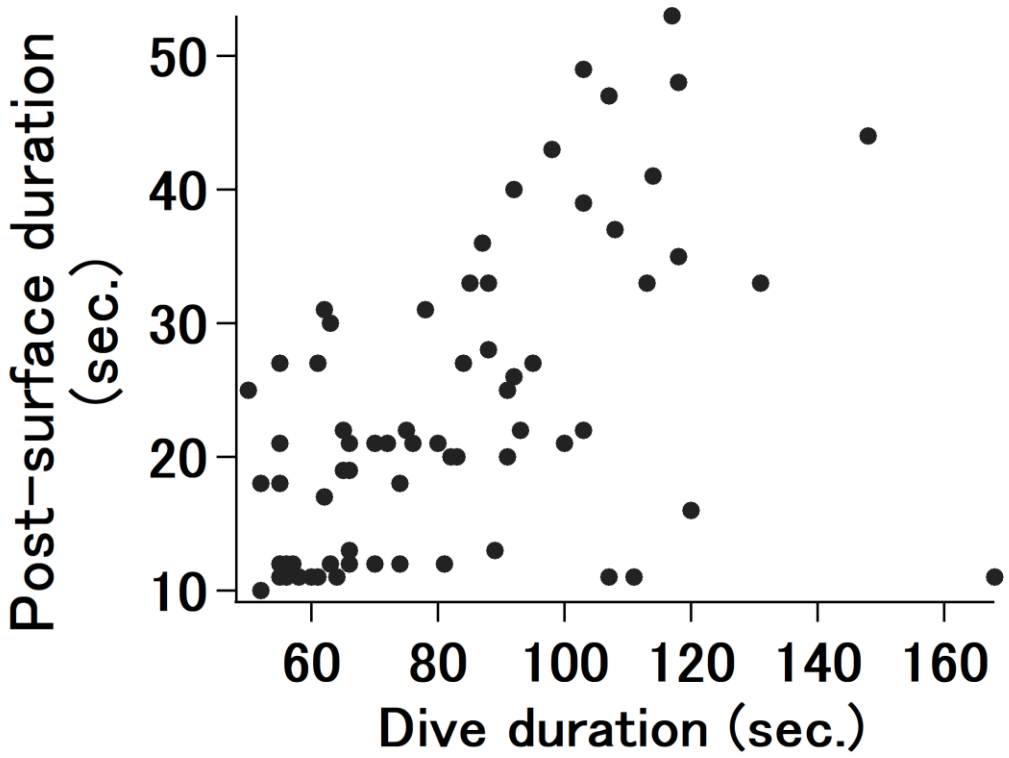

Figure 2-12. Relationship between dive duration and post-surface duration of dives with greater than or equal to two lunges. This showed positive relationship (Pearson's $r = 0.52$, $p < 0.0001$, $R^2 = 0.27$; $n = 70$).

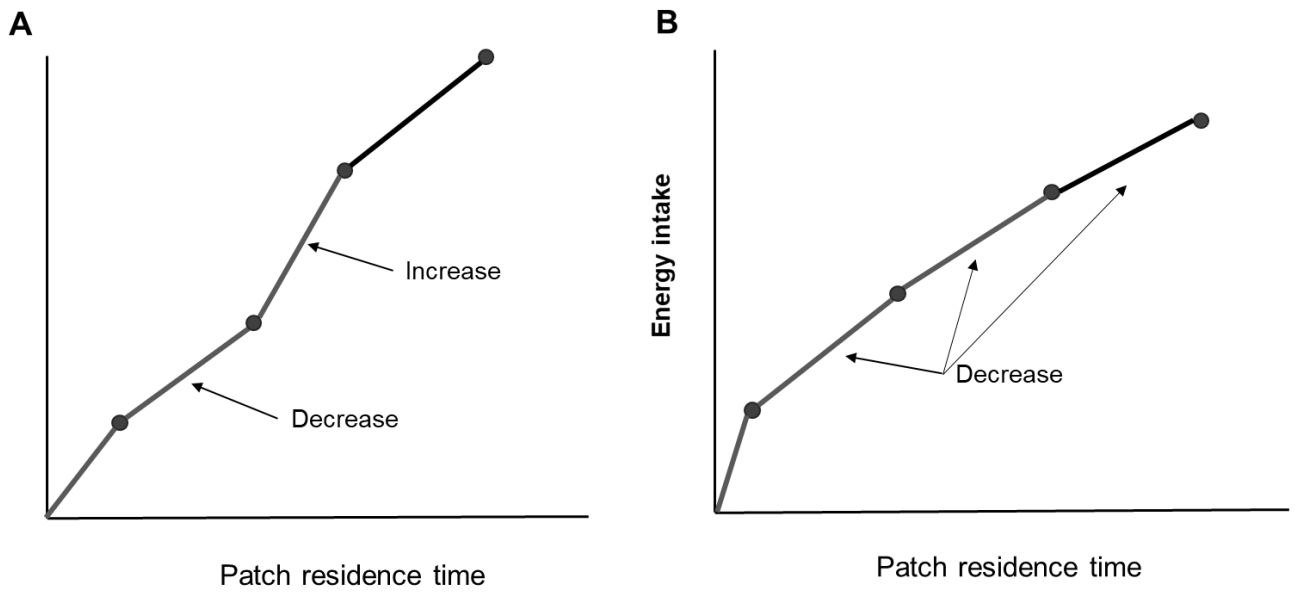

Figure 2-13. Illustrations showing the types of gain functions. (A) shows a decrease in energy intake at the second lunge but an increase at the third lunge. (B) shows a gradual decrease in rate of energy intake over lunges, observed in 90% of the dives.

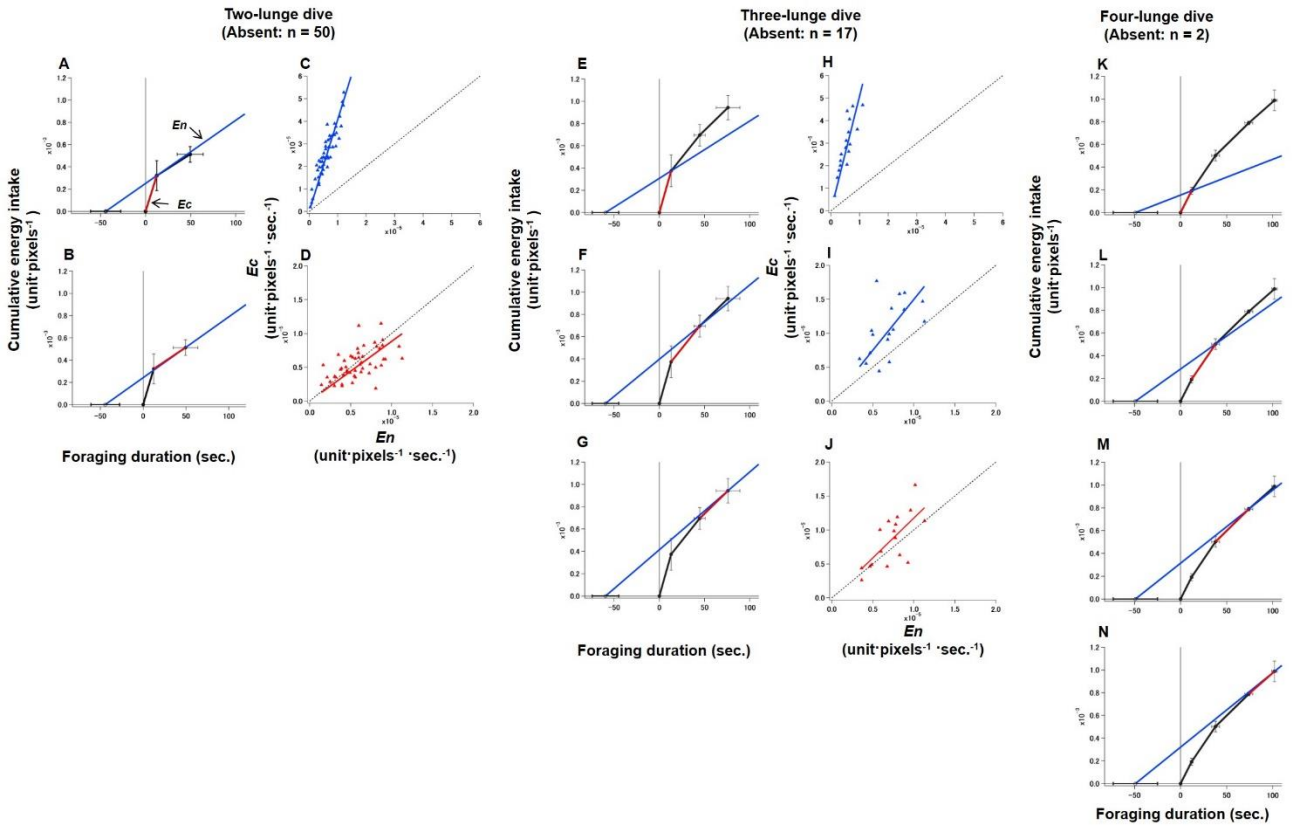

Figure 2-14. Foraging efficiency of each lunges. Foraging models comparing the total rates of energy intake (*En*) and gain functions using mean values of dives with (AB) two-lunges (n = 50), (E-G) three-lunges (n = 17), and (K-N) four-lunges (n = 2). X-axis shows the foraging duration, composed of transit (descent + ascent) + post-surface + patch residence time. Y-axis shows cumulative energy intake. The total rate of energy intake (*En*) up to each lunge is represented by a blue line, and the rate of energy intake in each lunge (*Ec*) is indicated by a black or red line. Error bars on the black dots and the starting point of the blue line (*En*) represent the standard deviation of the mean values. A linear regression model of *Ec* versus *En* (CDHIJ) of the corresponding foraging model are shown on the right side of each foraging model. The dashed black line represents where *Ec*/*En* =1. (C), (H), and (I) had *Ec*/*En* values greater than one (C; *Ec*/*En* = 4.1, 95% CI. 3.8 - 4.3: H; *Ec*/*En* = 5.1, 95%

CI. 4.5 – 5.7: I; 1.5, 95% CI. 1.2 – 1.8). Although (J) also had *Ec*/*En* values greater than one the 95 CI included *Ec/En* =1 (*Ec*/*En* = 1.2, 95% CI. 0.99 – 1.3). (D) had *Ec*/*En* values less than one (*Ec*/*En* = 0.88, 95% CI. 0.75 – 0.98).

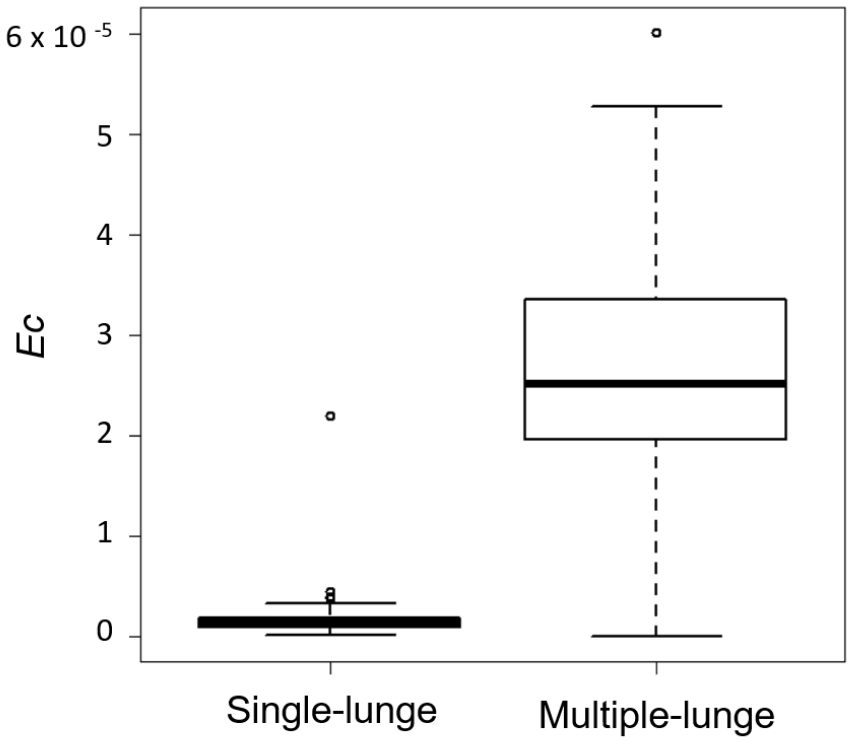

Figure 2-15. Comparison of *Ec* values of single lunge dives and first lunge of multiple lunge dives. The value of *Ec* for multiple lunge dives are significantly higher than that of single lunge dives. The maximum and minimum values are expressed by the whiskers, the boxes show the lower quartiles, the medians and the upper quartiles, and the circles are the outliers.

Figure 2-16. Snap shot from the video logger attached to a humpback whale. Another humpback whale swimming in front of the tagged whale.

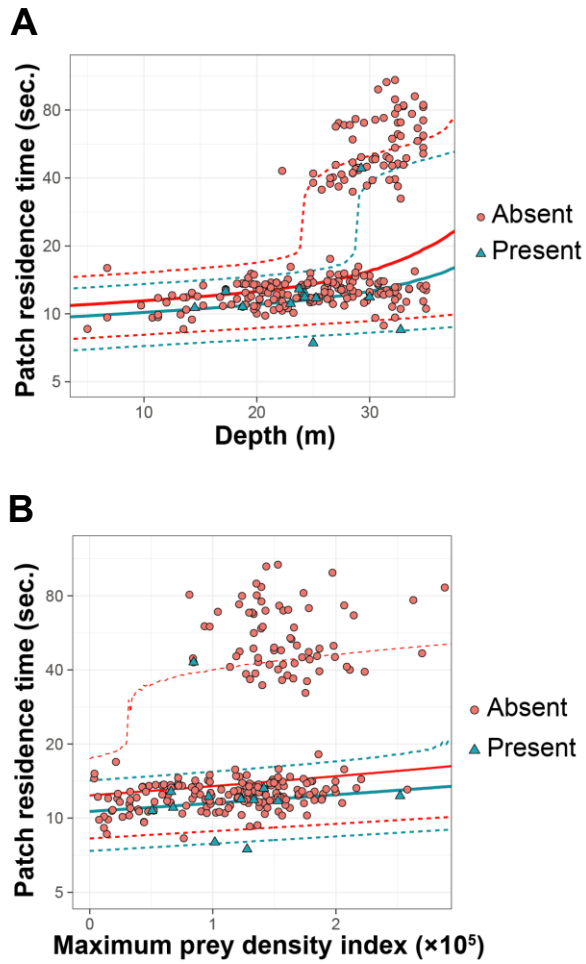

Figure 2-17. Relationships between patch residence time and (A) dive depth and (B) the maximum Index of Prey Density (IPD) for four whales. The red points represent absent (n = 232) dives and blue triangles represent present dives (n = 12). The points show the patch residence time, rescaled so that the effect of MIPD is normalized to its mean value in (a), and the effect of depth is normalized to its mean value in (b). The solid lines represent the mean values and the dashed lines represent the 95% prediction intervals of posterior distribution computed from the MCMC simulation. For computing 95% prediction intervals, MIPD was set to its mean value in (a) and depth was set to its mean value in (b).

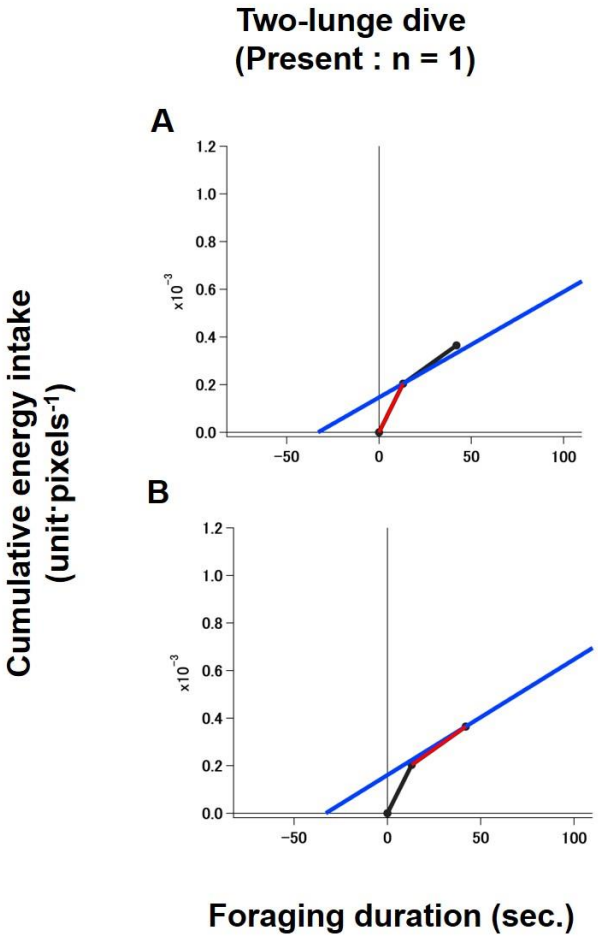

Figure 2-18. Foraging models comparing the total rates of energy intake (*En*) and gain functions using mean values of dives with two-lunges when other humpback whales are present (n = 1). (A) shows the total rate of energy intake (*En*) up to first lunge, represented by a blue line, and the rate of energy intake of first lunge (*Ec*) indicated by red line. (B) shows the total rate of energy intake (*En*) up to second lunge represented by a blue line, and the rate of energy intake of the second lunge (*Ec*) indicated by red line.

CHAPTER 3

Resting characteristics and strategy

Closed to public

CHAPTER 4

Difference in time allocation of activities among foraging locations

Closed to public

CHAPTER 5

Evaluation of wave drag on bottlenose dolphin from swimming effort

5.1. Background

Aquatic animals live in a medium 820 times denser and 55 times more viscous than air. These two properties of water greatly increase body drag (Davis 2014), thus costing the animal large amounts of energy during under-water locomotive activities such as swimming and diving (Berta et al. 2005).

Specifically, four types of hydrodynamic drag are known to be acting on marine mammals swimming at a constant speed: 1) friction drag, due to animal's wetted surface area and viscosity producing shear stresses in the boundary layer, 2) pressure drag resulting from displacement of water due to animal's body structure causing distortion of flow outside the boundary layer creating pressure gradients, 3) induced drag components, produced from pressure difference created by hydrofoils (fins, flippers or flukes) mammals use to generate thrust 4) and lastly, wave drag (Berta et al. 2005; Fish 1993). When an animal or an object travels along the water surface, due to increased area of water-air interface, the surrounding water is pushed out generating waves behind it. Thus, at the water surface, the work needed for wave generation, known as wave drag must also be considered in addition to frictional and pressure drag (Vogel 1994; Vennell et al. 2006). The dominant components of drag when submerged are frictional and pressure-related. Near the surface, wave drag is recognized to be the largest (Fish 1993; Vennell et al. 2006) and is estimated to be 5

times greater than the drag felt at a depth 3 times the body diameter (height), which reduces with depth and further becomes negligible (Heinrich 1966; Fish 1993; Hindle et al. 2010).

Cetaceans that need to return to the surface to breathe cannot avoid the effect of wave drag. However, by constantly repeating shallow dives at few meters below the surface when swimming, cetacean may avoid the effect of wave drag. The shallow dives of humpback whales observed around 10 to 20 meters in depth during the moving bout in chapter 4 may be a way for them to avoid wave drag near the surface. Previous studies have used mannequins to study the effect of wave drag on human swimmers (Vennell 2006) or estimated surface and submerged drag by towing a harbor seal in a gliding position using load cell (Williams and Kooyman 1985). However, no direct study has been reported on wave drag with animal swimming by its own effort. Therefore, by attaching animal-borne accelerometer to a dolphin trained to swim horizontally at the water surface and at predefined depths, the effect of wave drag was estimated from the dolphin's stroking effort and the swim speed achieved by the animal while swimming by its own effort. If wave drag exerts a significant impact on swimming dolphins, stroke effort of dolphin swimming at the same speed is expected to be larger at the surface than below.

5.2. Materials and methods

5.2.1. Experimental procedure

A male bottlenose dolphin *Tursiops truncatus* from Minamichita Beachland Aquarium in Aichi prefecture, Japan, was used for this study. The dolphin with a body length of 2.99 m, height of approximately 0.7 m, and mass of 289 kg, was trained for 3 months (Fig. 5-1A).

The study was conducted in a pool at the Minamichita Beachland Aquarium with dimensions of approximately 30 m width, 15 m length, and 3.5 m depth at the deepest point (Fig. 5-1B). The experiment was conducted for a total of 9 days between February and May 2013, with 2 to 3 sessions a day during the morning feeding time, between aquarium shows at daytime and the last feeding time in the afternoon. The number of trails per session depended on the animal's concentration and amount of fish left to feed for the day.

The dolphin was trained to swim horizontally at the surface and at depths of 3 m, which is approximately 4 times the body height. For surface trail, the dolphin was trained to follow the trainer running along the edge of the pool. Its dorsal fin was always out of the water during surface trails. For 3-m trails, two sets of poles with a target attached at the end were used and were fixed at the depth of 3 m (Fig. 5-1C). The dolphin dove down and touched the first target with its rostrum and swam between the poles keeping a constant depth, then touched the other target and came up to the surface. To kill the momentum when diving, the dolphin was trained to stop at the first target for few

seconds. Due to the limited area of the pool, the distance for surface trail and 3-m trail was approximately 20 m and 13 m, respectively.

5.2.2. Instruments

In this study, two types of animal-borne recorders (hereafter, accelerometer) W190L-PD3GT (22 mm in diameter, 114 mm in length, 60 g in air, Little Leonardo Corp., Tokyo, Japan) and W1000-3MPD3GT (26 mm in diameter, 175 mm in length, 140g in air, Little Leonardo Corp., Tokyo, Japan) were used to quantify the animal's speed, stroking effort, and depth. W190L-PD3GT was programmed to record 3-axis acceleration at 32 Hz, speed at 8 Hz, and depth at 1-Hz intervals. W1000-3MPD3GT was programmed to record tri-axis acceleration at 32 Hz, speed and depth at 1 Hz. Each accelerometer was mounted directly on a black rubber suction cup (85 mm in diameter, Canadian Tire Corporation., Canada) used to attach the accelerometer to the dolphins' body by landing the dolphin on the pool side (Fig. 5-1A, Fig. 5-2).

The speed of an animal was recorded as the rotation counts of propeller mounted on the accelerometer. W190L-PD3GT accelerometers was first used, which is smaller and considered to have less drag and effect on the dolphin. However, high speed swimming of the dolphin was too fast for the sensor to detect rotation counts of the propeller. Therefore, three blades were cut off from the propeller customarily consisting six blades and the nut was tightened before every session in order to decrease the propeller's rotation. Thus, this accelerometer needed to be calibrated after every session

using the dolphin. The dimensions of the pool were measured and had the dolphin swim around the pool at high speed. This “high-speed swim” was video-recorded from above using GoPro HERO3+ (GoPro., USA) and the speed of dolphin was calculated from the GoPro video recording. Conversion equation was obtained using calculated speed and the rotation number of the propeller. Regression coefficients for this method were relatively high, at 0.998 (n = 4). The adjustment of the propeller of W190L-PD3GT accelerometer was a challenge and only a couple of successful data were obtained, therefore, used W1000-3MPD3GT accelerometer instead. No adjustment of the propeller was needed for W1000-3MPD3GT accelerometer, and rotation counts were converted to speed with the equation obtained from the calibration experiment using an experimentally designed water flow tunnel. Accelerometers were set inside the tunnel and rotation counts were obtained from flow speed ranging from 0.1 to 1.1 $m \cdot s^{-1}$ to plot a regression line. Regression coefficient was 0.999 (n = 10).

5.2.3. Data analysis

The effect of wave drag was assessed from the swimming effort of the dolphin, such as stroke frequency and body amplitude. Time-series data obtained from the accelerometers were analyzed using *IGOR Pro* (WaveMetics, Inc., Lake Oswego, OR, USA). Among the three axes of acceleration, dorso-ventral axis (Fig. 5-1A) was used for calculating the stroke frequency. The acceleration sensor of the data logger measures both, gravity-based acceleration and specific acceleration related to

propulsive activity (Tanaka et al. 2001; Sato et al. 2003); the latter was used for stroke analysis. The dominant stroke frequency of every independent session was determined by calculating the power spectral density (PSD) of the dorso-ventral axis (Fig. 5-3). PSD results showed an obvious peak around 2 Hz which is believed to be the dominant stroke cycle frequency (Sato et al. 2007) and 2 troughs around 1 and 3 Hz. The smallest value of trough from all sessions was 0.7 Hz and the highest value was 3.4 Hz. Thus, in order to separate the stroking events from other movements, frequencies lower than 0.7 Hz and higher than 3.4 Hz were filtered (IFDL Version 3.1, WaveMatrics, Inc., USA). From the data, peaks with absolute amplitude greater than values ranging from 0.39 to 0.69 m s^{-2} were extracted as strokes and a set of up-and-down durations was considered as a single flipper stroke. The number of strokes of each trail was then divided by the duration of the trail to obtain stroke frequency (Hz).

Dolphins generate thrust by oscillating their fluke and are known to oscillate their entire body while swimming (Fish and Hui 1991; Williams et al. 1999). Because the amplitude of the fluke oscillation could not be measured, dorso-ventral amplitude of the body oscillation "*A*" was used in the analysis. The measured dorso-ventral acceleration (m s^{-2}) was integrated twice to obtain the position of the body (m). The position of the body oscillated and the mean amplitude of the body oscillation (*A*) in meters for each trail was used for analysis (Fig. 5-4).

When animals are swimming horizontally in a uniform linear motion, thrust and drag is balanced. In order to determine whether dolphins swam in a uniform linear motion, speed was differentiated

and the trails of value with high absolute acceleration were not used for analysis.

5.2.4. Statistical analysis

Single-factor ANOVA was used in order to compare swimming effort between the surface and at 3 m as previously described by Zar (1999). Values for significance were set at $P < 0.05$.

5.3. Results

5.3.1. General swimming performance

During the nine days of experiment, 23 sessions were conducted and 12 of them were used for analysis. The remaining 11 sessions could not be used as they lacked speed data due to problems with the propeller. The distribution of mean absolute acceleration of all trails within the 12 sessions was plotted (Fig. 5-5). Values of acceleration higher than 1.0 m s^{-2} were not used for analysis because the dolphins are less likely to be swimming at uniform linear motion during these sessions. Thus, data from 15 trails of 3-m and 16 trails of the surface were used for analysis. The mean values of speed, stroke frequency, and body amplitude for experiments are indicated in Table 5-1.

5.3.2. Stroke frequency and body amplitude

The dolphin's swim speed could not be controlled, and speed range differed between the

values observed at the surface and at 3 m. Thus, in order to statistically compare the difference in swimming effort at these 2 depths, speed data within the range of 2.65 $m \cdot s^{-1}$ and 3.35 $m \cdot s^{-1}$ (surface: n = 13, 3 m: n = 11) was only used so there would be no significant difference between speed at the surface and at 3 m (ANOVA, $F_{(1,1,23)} = 2.005$, $P = 0.171$; Fig. 5-6A). The swimming effort at the surface and at 3 m indicated no significant difference in stroke frequency (ANOVA, $F_{1,23} = 3.02$, $P = 0.096$; Fig. 5-6B) but significantly greater body amplitude at surface (ANOVA, $F_{1,23} = 10.5$, $P < 0.05$; Fig. 5-6C).

5.4. Discussion

In this experiment, no significant difference between stroke frequency was observed at the surface and at 3 m, however a difference was noted in body amplitude within the same speed range. This indicates that dolphins can achieve the same speed with less effort at deeper depths, which suggests that there is an effect of wave drag at surface.

This study enabled to detect the effect of wave drag, although, the results showed only a slight difference between values observed at the surface and at 3 m and were not clear enough for quantitative analysis. There are several reasons which may account for this result. One is the morphological features of the dolphin which are highly adapted to aquatic activity. Fineness ratio (FR), a measure of body streamlining for dolphins approaches the optimum value of 4.5, which represents the lowest drag ratio of maximum body volume to minimum surface area (Fish and Hui

1991; Berta 2005). Thus, it is more likely that the effect of wave drag on dolphins will be less than the commonly stated estimate of drag being 5 times greater at surface than below a depth of 3 times the body diameter, obtained by towing a dead pike with a soft and flexible body, (Heinrich 1966). In fact, a study using harbor seal having similar FR as dolphins indicated only a 2.5-fold increase as compared to the submerged value at the surface, at a speed of 2.0 $m \cdot s^{-1}$ (Williams and Kooyman 1985).

Another reason may be the speed ranges. William et al. (1993) indicated that heart rate, respiration rate, and post-exercise blood lactate concentration of the bottlenose dolphin swimming horizontally at constant speed below 1 m from the surface showed no significant difference until it approached a speed of 2.9 $m \cdot s^{-1}$. The dolphins were to swim at their favorable speed at 3 m trail where the mean swim speed was 2.8 ± 0.3 $m \cdot s^{-1}$. If speed was increased over 2.9 $m \cdot s^{-1}$, there may have been a clearer trend of change in swimming effort with speed between surface and at 3 m.

Lastly, depth may be another reason. The experiments were performed in shallow water, about 3.5 m at the deepest point. Theoretically, 3 m is more than 3 times the body diameter of the dolphin, therefore, the water level was deep enough to reduce the effect of wave drag by one-fifth based on previous knowledge. However, in this circumstance, during 3-m trails the dolphin was swimming very close to the bottom; this might have physically affected the dolphins' swimming characteristics, such as swimming postures and stroke amplitude. Furthermore, there could have been different aspects of drag acting on the swimming dolphin, for instance, waves reflecting back from the bottom

of the pool. In either case, better-controlled experimental design is required for further understanding on the effect of wave drag on swimming animals.

Though, in the case of wild humpback whales, the body diameter of humpback whale is reported to be 3.21 meters (Woodward et al. 2006). Three times this body diameter will be around 10 meters, a depth where effect of wave drag is estimated to be insignificant for humpback whales. This completely matched with the depth which wild humpback whales were frequently using. Hence, it is very likely that during dives of moving bouts, humpback whales are frequently using the depth around 10 to 20 meters where the effect of wave drag is estimated to be insignificant.

Table 5-1. Mean values of swim speed and swimming efforts obtained from experiment at the pool. Values are mean ± SD.

Trails	Speed ($m \cdot s^{-1}$)	Stroke frequency (Hz)	Body amplitude ($10^{-2} \times m$)
3 m (n = 15)	2.8 ± 0.3	1.7 ± 0.3	1.4 ± 0.4
Surface (n = 16)	3.2 ± 0.2	1.9 ± 0.2	1.8 ± 0.4

A

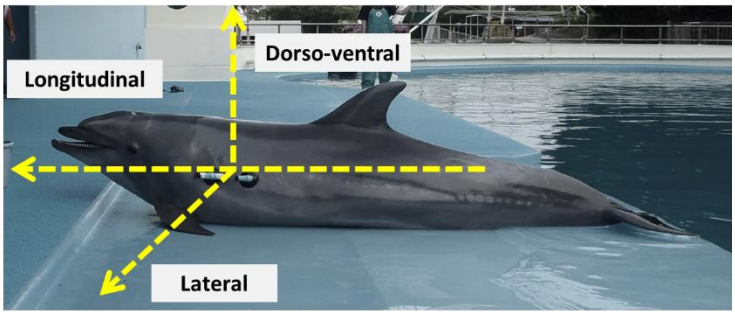

B

C

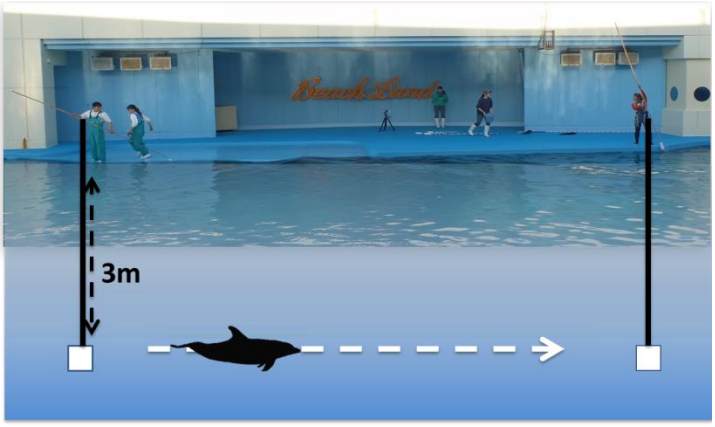

Figure 5-1. (A) Direction of 3-axis acceleration measured by an accelerometer. (B) Experimented pool of Minamichita Beachland Aquarium. (C) Experiment procedure of 3 m trail.

Figure 5-2. W190L-PD3GT accelerometer with black suction cup

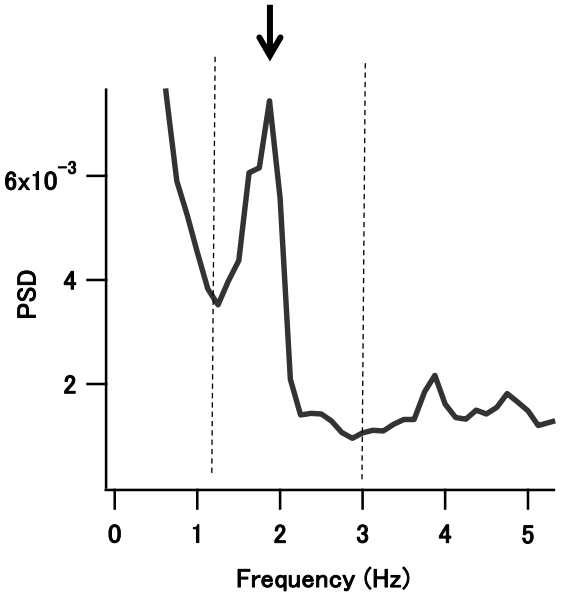

Figure 5-3. PSD result of dorso-ventral axis with arrow showing the peak around 2 Hz which is the dominant stroke frequency and the range within the lines are filtered to separate the stroking events from other movements.

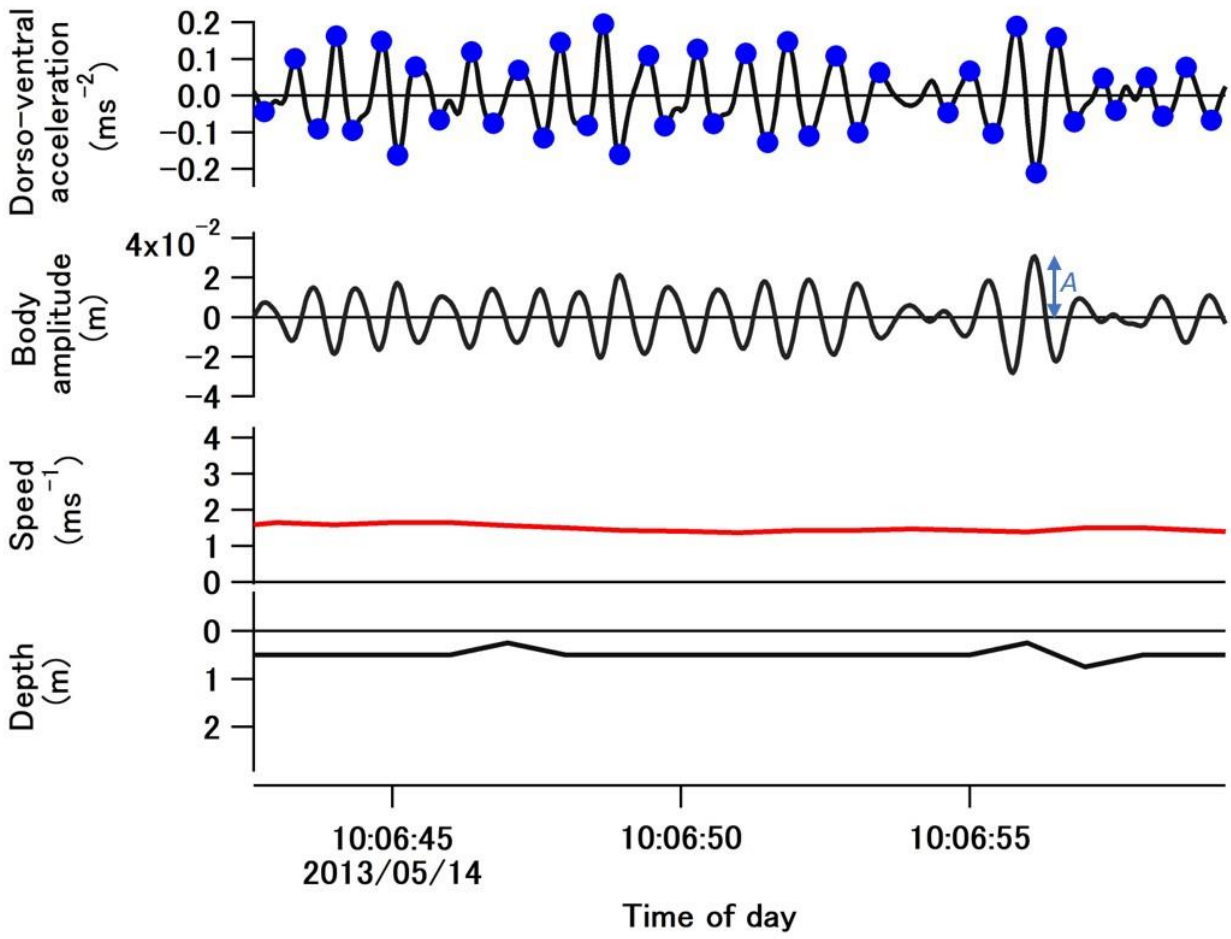

Figure 5-4. Time series data from experiment conducted for surface slow trail showing depth, speed, estimated body amplitude and dorso-ventral acceleration with stroke indicated in blue dots.

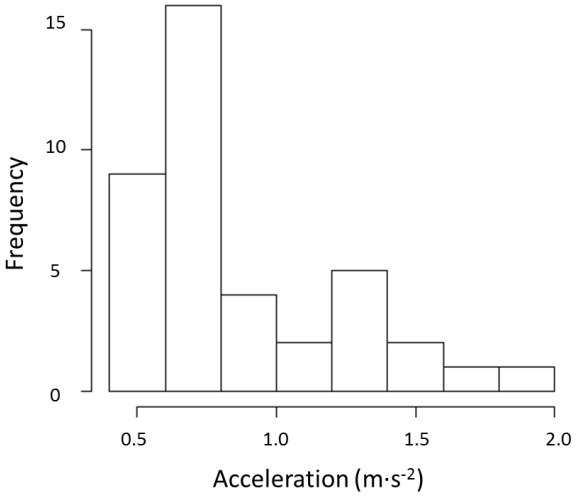

Figure 5-5. Distribution of mean absolute acceleration in speed for all trails.

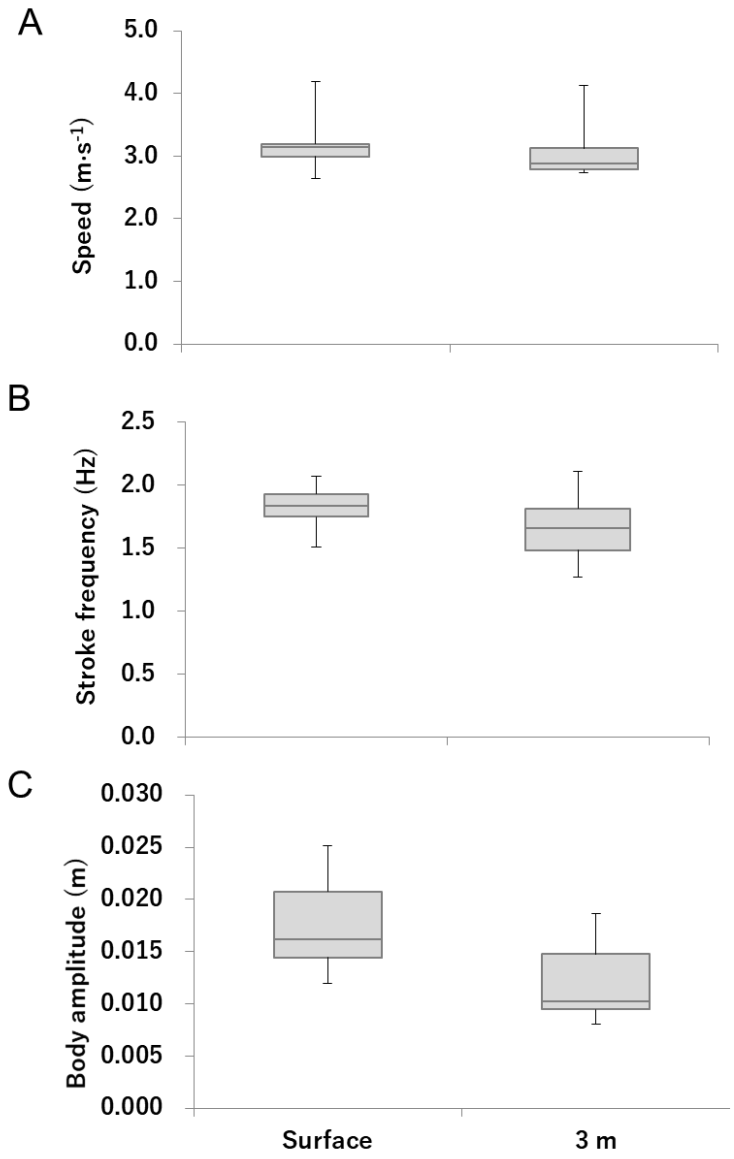

Figure 5-6. Box plots of speed (A) stroke frequency (B) and body amplitude (C) of surface and 3 m trail of the same speed range.

CHAPTER 6

General discussion

This study focused on activity patterns and time budget of the humpback whales in Iceland, Norway and Canada which is significant in two ways. Over-exploitation of whales during the eighteenth and nineteenth-century greatly reduced the number of humpback whales. Although, in effect of various conservation and protection acts, the number of humpback whales shows a recover. Currently, out of 14 distinct population, one is listed as threatened and four are still listed as endangered species and the populations foraging in Iceland and Norway in this study may include population still categorized as endangered species. Furthermore, conducting the study during the foraging period is important because humpback whales reduce the energy intake or completely stop feeding when they leave the foraging grounds (Berta et al. 2005), so the key to survival and fitness depend largely on how efficiently they gain energy during this period. Thus, studying the behavior of humpback whales during the foraging period may be a valuable information for conservation and management of these populations.

Foraging and resting are the two important behaviors for humpback whales during the foraging period. There were always difficulties to quantitatively analyze these behaviors of large wild animals especially living underwater. Although by attaching an accelerometer and a video camera directly to humpback whales, this study succeeded to quantitatively analyze these behaviors and added many new insights in terms of their foraging and resting behaviors.

There were many new attempts in chapter two. Even with the improvements in technology of animal-borne accelerometers and video loggers, obtaining the temporal change in prey density around marine predators is still challenging. This study, perhaps, is the first to estimate the change in prey density in front of a humpback whale in time and place where feeding occurred and explored the foraging efficiency of humpback whales in response to the changing prey density in a single dive using a model based on the central place foraging theory (CPF). While many studies fulfill the unknown parameters with assumption, the result of this study is purely derived from data taken from free-ranging humpback whales. This was only possible with the biggest attempt to estimate the prey density using a video-logger attached directly to a humpback whale. The results provided an exceptionally strong fit to the theoretical predictions of CPF, with a diminishing rate of energy intake over consecutive feeding events, and humpback whales efficiently fed by bringing the rate of energy intake close to maximum in a single dive cycle. Unexpectedly, this video-based method enabled to detect the presence of other humpback whales while foraging. An interesting trend of shortened patch resident time was observed when other humpback whales were feeding in the same patch. Thus, this present method may be an effective way to quantitatively investigate the predator–prey–competitor interactions for future studies.

The limitation of this method using video cameras was the narrow field-of-view, with information on prey being restricted to proximity in front of the whales, due to poor water clarity and limited light at greater depths. At shallow depths, the light condition was constant at all time of the

day, because this study was conducted during the season of midnight sun. The placement of the tag might also differ in each tagging attempt and over time, because the tags shift. As a result, it was not possible to estimate the prey density from the same angle-of-view. Still, in most cases, the tag shifted after attachment to be aligned with the water flow facing forward; thus, it was assumed that the levels of krill flowing by the whales as they swam through the patch reflected the quality of the patch, regardless of where the camera was attached. The quality of this method is not enough to estimate the absolute prey density or precise consumption rate. However, the most important part of this study was not to estimate the actual energy intake, but to identify the shape of the gain function. Stephens and Krebs (Stephens and Krebs 1986) stated the importance of specifying the energy intake over time, as this information determines the shape of the gain function, otherwise, foraging models are meaningless. Present method could simultaneously obtain the levels (high or low density) of prey information in front of the whale and the time that the feeding occurred. The shape of gain functions plotted using the data from this method should provide a good reflection of the relative energy intake of the whales over their patch residence time, allowing to investigate foraging dive efficiency. Thus, this approach may be the most effective and the only way to complete such a study based on existing technology. This study can be further improved by combining the method using an echo-sounder, giving us the information of both short-term and long-term change in prey density and distribution over time. Moreover, there have been vast improvements in technology over the past couple of years and some researchers are starting to use 360° cameras. This could resolve many of the issues in this

study, giving us better estimation of change in prey density and the observation of other animals around the tagged whale from all directions.

Humpback whales are frequently observed floating motionless at the surface which is often called “logging”, referred as their resting behavior (Lyamin et al. 2008). Furthermore, humpback whales are observed to perform long dives emerging from almost the same place for respiration which people believed that they are resting underwater (Robbins et al. 1998). In Chapter three, this logging behavior and underwater resting behavior of wild humpback whales in the feeding ground was quantitatively identified using data-loggers. This study perhaps is the first quantitative evidence that humpback whales rest motionless underwater by maintaining neutral buoyancy via controlling air volume in their lunges. As it is said, sleep evolved in the natural world. Species-specific sleep is believed to be shaped by the environmental factors (Allison and Cicchetti 1976; Rattenborg et al. 2017). This study indicated that resting (sleep-like behavior) of humpback whales are likely to be affected by the environmental condition. The increase in wind speed causing wave action at the surface may derive humpback whales to rest underwater in order to avoid the unstable condition at surface. Moreover, paper indicated that humpback whales are frequently observed logging at the surface when water is calm (Lyamin et al. 2008; Wright et al. 2016).

The exact position of where the humpback whales were resting could not be identified from datasets of this study. If this could be obtained, more detailed investigation could be made in terms of environmental factors that may affect the resting behavior of humpback whales other than wind

speed. Vessel-strikes is considered as a threat to humpback whales (Rus 2002; Berta et al. 2005). During rest, the level of consciousness decreases, increasing the risk of vessel-strikes (Izadi et al. 2018). A study with Risso's dolphins (*Grampus griseus*) also showed shift in resting time between high and low whale watching season (Visser et al. 2011). In all study sites, there were heavy traffic of fishing ships and whale watching boats at the surface especially during the day. This may derive humpback whales to rest underwater or move away to some area where people cannot reach.

Chapter 4 discussed the activity pattern and time budget of humpback whales during the foraging period. Understanding how an individual animal allocates time between various activities is important, as this can help us understand both ecological and physiological constraints on animals and its influence on fitness (Christiansen et al. 2015). Different behavioral patterns will be optimal during different condition because behavioral patterns are determined by internal variables related to the motivational state of an individual, and external variable related to the environment (Christiansen et al. 2015). Present study showed variation in time budget among locations. Large proportion of time was spent on foraging for humpback whales in Iceland and Canada but not for ones in Norway. As described in chapter 4, difference in tagging season and prey type were addressed as a reason for variation in time budget among location. But among the two, the seasonal difference can be better explained from our current data set, accounting to the motivational state of an individual to accomplish it goal, which is to store enough energy. Humpback whales during the early foraging season (Iceland, Canada) spent more time for foraging, whereas humpback whales during the late

foraging season spent less time for foraging (Norway) because they had stored enough energy. This strategy seems very reasonable, but the result of resting bout duration and moving bout duration was rather unexpected. Investigation of time budget and activity pattern of diurnal animals showed that they spent majority of daylight hours in two principle activities, foraging and resting (Herbers 1981). Whether humpback whales are diurnal or nocturnal is unknown, due to uneven duration of data (Fig. 4-4E). Still, it was expected that the two principle activities for humpback whales would also be foraging and resting, with foraging taking larger proportion of their time budget since they have higher demand for feeding during the foraging season. However, the two principle activities for humpback whales in foraging grounds were foraging and moving, and the most surprising result was how humpback whales can reduce their resting to this extent. Because the duration of resting was so short, statistical analysis did not indicate the trade-off relationship between foraging duration and resting duration, but it is still likely that foraging demand is reflecting the short resting duration. Bryde's whales are same baleen whale as humpback whales which feed on same type of prey with generally the same feeding strategy. However, a study indicated that bryde's whale rest entirely at night (Izadi et al. 2018). The difference between humpback whales and bryde's whales is that bryde's whales do not undergo long distance seasonal migration and their feeding is not restricted to certain period of the year which indicates that they do not have extreme restriction, therefore; have less demand for foraging. Izadi et al. (2018) also raised this point as a reason for their long resting duration. Comparing these two species show how special humpbacks whales are in terms of activity

patter and time budget.

Overall, in all activities, depth selection played a key role to their activity patterns. Deep dives were rare in humpback whales and all activities with few exceptions basically occurred within 50 meters. This study suggested that humpback whales always selected the most efficient depth for each activity perhaps in terms of cost of transport. For foraging, humpback whales generally fed at shallow depth of an average of 25.1 ± 7.0 m. Previous study indicated that humpback whales did not feed during the daytime where they observed the highest prey density in depth but rather fed on krill that migrated at shallow depth at night. The vertical distribution of prey patch is unknow with this study, thus whether or not there was a better prey patch at deeper depth in unknown. Although this study showed that within 35m humpback whales were frequently feeding at depth abundant in prey.

Indication of depth selection with dives during moving bouts were also observed, where humpback whales frequently used depth around 10 to 20 meters. This phenomenon was hypothesized to be associated with the effect of wave drag on animal at surface. In chapter five, experimental study using trained bottlenose dolphins was conducted to assess the effect of wave drag on swimming cetacean. The study indicated that dolphin with a body diameter of 0.7 m can swim with less effort at 3 m in depth than surface where the effect of wave drag is estimated to be less. As for humpback whales the effect of wave drag is estimated to be insignificant around 10 m which matched with the depth they were frequently using, suggesting that humpback whales constantly repeated shallow dives around 10 to 20 m when moving to avoid the effect of wave drag at surface. Lastly, the finding

of depth selection of resting behavior was most remarkable as it does not seem to matter as much compared to other activities which involves movement. But again, humpback whales were selecting the most comfortable and relevant depth to avoid unfavorable force such as unstable condition at surface.

Future perspective

Some long-term monitoring of humpback whales in Gulf of St Lawrence, Canada showed a shift in timing of migration of humpback whales due to climate-induced change in resource, causing increased temporal overlap with the fin whales which also migrate to feed at the same gulf (Ramp et al. 2015). The researchers are concerned that the temporal separation that was maintained between the two species are starting to erode and increase competition affecting their fitness in the future. Accumulating the information on behavior of humpback whales will help us identify the changes or abnormal behavior that may affect their fitness as reported in Canada, therefore; is very important for the conservation and management of the animal itself. Moreover, understanding the behavior of humpback whales can lead to understanding the marine ecosystem. Identifying the foraging behavior and predator-prey interaction of top predators has recently been used as an index of monitoring the ecosystem (Piatt et al. 2007). As a major consumer of worldwide oceanic productivity, humpback whales will be a powerful tool for monitoring the whole marine ecosystem and allow us to understand how animals share the resource in an environment.

Literature cited

Acevedo J, Plana J, Aguayo-lobo A, Pastene LA. 2011. Surface feeding behavior of humpback whales in the Magellan Strait. Rev Biol Mar Oceanogr. 46(3):483–490.

Akamatsu T, Rasmussen MH, Iversen M. 2014. Acoustically invisible feeding blue whales in Northern Icelandic waters. J Acoust Soc Am. 136(2):939–944.

Allison T, Cicchetti D V. 1976. Sleep in mammals: Ecological and constitutional correlates. Science 194(4266): 732-734.

Berta A. 2015. Whales, dolphins &porpoises: Anatural history and Species guide. Whitehead M, Kitch T, Earle C, Shanahan Kate, editor. United Kingdom: The Ivy Press Limited.

Berta A, Sumich JL, Kovacs KM. 2005. Marine mammals: Evolutionary biology. Second Edition. San Diego: Academic Press, Elsevier.

Cade DE, Friedlaender AS, Calambokidis J, Goldbogen JA. 2016. Kinematic diversity in rorqual whale feeding mechanisms. Curr Biol. 26(19):2617–2624.

Campbell SS, Tobler I. 1984. Animal sleep: A review of sleep duration across phylogeny. Neurosci Biobehav Rev. 8(3):269-300.

Christiansen F, Lynas NM, Lusseau D, Tscherter U. 2015. Structure and dynamics of minke whale surfacing patterns in the gulf of St. Lawrence, Canada. PLoS One. 10(5):e0126396.

Clapham PJ. 1996. The social and reproductive biology of humpback whales: An ecological perspective. Mamm Rev. 26(1):27–49.

Clapham PJ, Mayo CA. 1987. Reproduction and recruitment of individually identified humpback whales, *Megaptera novaeangliae*, observed in Massachusetts Bay, 1979-1985. Can J Zool. 65:1065–1066.

Davis RW. 2014. A review of the multi-level adaptations for maximizing aerobic dive duration in marine mammals: from biochemistry to behavior. J Comp Physiol B. 184(1):23–53.

Doniol-Valcroze T, Lesage V, Giard J, Michaud R. 2011. Optimal foraging theory predicts diving and feeding strategies of the largest marine predator. Behav Ecol. 22(4):880–888.

Ebensperger LA, Hurtado MJ. 2005. Seasonal changes in the time budget of degus, *Octodon degus*. Behaviour 142(1):91–112.

Fish FE. 1993. Power output and propulsive efficiency of swimming bottlenose dolphins (*Tursiops truncatus*). 193:179–193.

Fish FE, Hui CA. 1991. Dolphin swimming–a review. Mamm Rev. 21(4):181-195.

Foo D, Semmens JM, Arnould JPY, Dorville N, Hoskins AJ, Abernathy K, Marshall GJ, Hindell MA. 2016. Testing optimal foraging theory models on benthic divers. Anim Behav. 112:127–138.

Friedlaender AS, Hazen EL, Goldbogen JA, Stimpert AK, Calambokidis J, Southall BL. 2016a. Prey-mediated behavioral responses of feeding blue whales in controlled sound exposure experiments. Ecol Appl. 26(4):1075–1085.

Friedlaender AS, Johnston DW, Reny B, Kaltenberg A, Goldbogen JA, Stimpert AK, Curtice C, Hazen EL, Halpin PN, Read AJ, et al. 2016b. Multiple-stage decisions in a marine central-place forager. R Soc Open Sci. 3(5):160043.

Gambell R. 1993. International management of whales and whaling: An historical review of the regulation of commercial and aboriginal subsistence whaling. ARCTIC. 46(2):97–107.

Goldbogen JA., Hazen EL, Friedlaender AS, Calambokidis J, DeRuiter SL, Stimpert AK, Southall BL. 2015. Prey density and distribution drive the three-dimensional foraging strategies of the largest filter feeder. Funct Ecol. 29(7):951–961.

Goldbogen JA, Calambokidis J, Croll DA, Harvey JT, Newton KM, Oleson EM, Schorr G, Shadwick RE. 2008. Foraging behavior of humpback whales: kinematic and respiratory patterns suggest a high cost for a lunge. J Exp Biol. 211(23):3712–3719.

Goldbogen JA, Calambokidis J, Oleson E, Potvin J, Pyenson ND, Schorr G, Shadwick RE. 2011. Mechanics, hydrodynamics and energetics of blue whale lunge feeding: efficiency dependence on krill density. J Exp Biol. 214(1):131–46.

Goldbogen JA, Calambokidis J, Shadwick RE, Oleson EM, McDonald MA, Hildebrand JA. 2006. Kinematics of foraging dives and lunge-feeding in fin whales. J Exp Biol. 209(7):1231–44.

Goldbogen JA, Shadwick RE, Pyenson ND. 2007. Big gulps require high drag for fin whale lunge feeding. Mar Ecol Prog Ser. 349:289–301.

Halle S, Stenseth NC. 2000. Activity patterns in small mammals: An ecological approach. Springer-Verlag Berlin Heidelberg.

Hazen E, Friedlaender A, Thompson M, Ware C, Weinrich M, Halpin P, Wiley D. 2009. Fine-scale prey aggregations and foraging ecology of humpback whales *Megaptera novaeangliae*. Mar Ecol Prog Ser. 395:75–89.

Hazen EL, Friedlaender AS, Goldbogen JA. 2015. Blue whales (*Balaenoptera musculus*) optimize foraging efficiency by balancing oxygen use and energy gain as a function of prey density. Sci Adv. 1(9):e1500469.

Heinrich H. 1966. Structure Form and Movement. New york: Reinhold Publishing Corporation.

Herbers JM. 1981. Time resources and laziness in animals. Oecologia. 49(2):252-262.

Hindle A, Rosen D, Trites A. 2010. Swimming depth and ocean currents affect transit costs in Steller sea lions *Eumetopias jubatus*. Aquat Biol. 10:139–148.

Houston AI, Carbone C. 1992. The optimal allocation of time during the diving cycle. Behav Ecol. 3(3):255–265.

Huang C, Wei F, Li M, Li Y, Sun R. 2003. Sleeping cave selection, activity pattern and time budget of white-headed langurs. Int J Primatol. 24(4):813-824.

IWC. Whale population estimates. [accessed 2018 Nov 25]. https://iwc.int/estimate.

Izadi S, Johnson M, de Soto NA, Constantine R. 2018. Night-life of Bryde's whales: ecological implications of resting in a baleen whale. Behav Ecol Sociobiol. 72(5):1-12.

Johnson MP, Tyack PL. 2003. A digital acoustic recording tag for measuring the response of wild marine mammals to sound. IEEE J Ocean Eng. 28(1):3-12.

Kooyman GL, Ponganis PJ. 1998. The physiological basis of diving to depth: birds and mammals. Annu Rev Physiol. 60(1):19–32.

Lea SEG, Daley C, Boddington PJC, Morison V. 1996. Diving patterns in shags and cormorants (*Phalacrocorax*): Tests of an optimal breathing model. Ibis. 138(3):391-398.

Lyamin OI, Manger PR, Ridgway SH, Mukhametov LM, Siegel JM. 2008. Cetacean sleep: An unusual form of mammalian sleep. Neurosci Biobehav Rev. 32:1451–1484.

Lyamin OI, Shpak OV, Nazarenko EA, Mukhametov LM. 2002. Muscle jerks during behavioral sleep in a beluga whale (*Delphinapterus leucas* L.). Physiol Behav. 76(2):265-270.

McNamara JM, Houston AI. 1985. Optimal foraging and learning. J Theor Biol. 117(2):231–249.

Miller PJO, Aoki K, Rendell LE, Amano M. 2008. Stereotypical resting behavior of the sperm whale. Curr Biol. 18(1):21–23.

Minamikawa S, Naito Y, Sato K, Matsuzawa Y, Bando T, Sakamoto W. 2000. Maintenance of neutral buoyancy by depth selection in the loggerhead turtle *Caretta caretta*. J Exp Biol. 203(Pt 19):2967–75.

Mori T, Miyata N, Aoyama J, Niizuma Y, Sato K. 2015. Estimation of metabolic rate from activity measured by recorders deployed on Japanese sea bass *Lateolabrax japonicus*. Fish Sci. 81(5):871–882.

Mori Y. 1998. Optimal choice of foraging depth in divers. J Zool. 245(3):249–283.

Mori Y and Boyd IL. 2004. The behavioral basis for nonlinear functional responses and optimal foraging in antarctic fur seals. Ecol. 85(2)398-410

Mori Y, Takahashi A, Mehlum F, Watanuki Y. 2002. An application of optimal diving models to diving behaviour of Brünnich's guillemots. Anim Behav. 64(5):739–745.

Mårtensson P-E, Gotaas ARL, Norddy ES, Blix AS. 2006. Seasonal changes in energy density of prey of northeast Atlantic seals and whales. Mar Mammal Sci. 12(4):635–640.

Mukhametov LM. 1987. Unihemispheric slow-wave sleep in the Amazonian dolphin, *Inia geoffrensis*. Neurosci Lett. 79(1-2):128-132.

Mukhametov LM, Supin AI. 1975. An EEG study of different behavioral states of freely moving dolphins. Zhurnal Vyss Nervn Deiatelnosti Im I P Pavlov. 25(2):396-401.

Mukhametov LM, Supin AY, Polyakova IG. 1977. Interhemispheric asymmetry of the electroencephalographic sleep patterns in dolphins. Brain Res. 134(3):581-584.

Narazaki T, Isojunno S, Nowacek DP, Swift R, Friedlaender AS, Ramp C, Smout S, Aoki K, Deecke VB, Sato K, et al. 2018. Body density of humpback whales (*Megaptera novaengliae*) in feeding aggregations estimated from hydrodynamic gliding performance. PLoS One 13(7):e200287.

Narazaki T, Shomi K. 2010. Reconstruction of 3-D path (ThreeD_path). Available: http://bre.soc.i.kyoto-u.ac.jp/bls/index.php?3D_path

NOAA. 2016a. Endangered and threatend species; Identification of 14 distinct population segments of the humpback whale (*Megatera novaeangliae*) and revision of species-wide listing. Fed Regist. 81(174):62260–62320.

NOAA. 2016b. Endangered and threatend species; Natl Ocean Atmos Adm. [accessed 2018 Nov 25]. https://www.fisheries.noaa.gov/species/humpback-whale.

Nowacek DP, Friedlaender AS, Halpin PN, Hazen EL, Johnston DW, Read AJ, Espinasse B, Zhou M, Zhu Y. 2011. Super-aggregations of krill and humpback whales in Wilhelmina bay, Antarctic Peninsula. PLoS One 6(4):e19173.

Orians, GH, Pearson N. 1979. On the theory of central place foraging. Analysis of Ecological System. Columbus, Ohio: Ohio State Universtiy Press. p. 154–177.

Orton LS, Brodie PF. 1987. Engulfing mechanics of fin whales. Can J Zool. 65(12):2898-2907.

Payne RS, McVay S. 1971. Songs of humpback whales. Science 173:585–597.

Piatt JF, Sydeman WJ, Wiese F. 2007. Introduction: A modern role for seabirds as indicators. Mar Ecol Prog Ser. 352:199–204.

Pierre-Henry F. 2007. Whales and Seals: Biology and Ecology. 3rd ed. Pennsylvania: Schiffer.

Pinet PR. 2009. Invitation to Oceanography. 5th, editor. Jones & Barlett.

Potvin J, Goldbogen JA, Shadwick RE. 2010. Scaling of lunge feeding in rorqual whales: an integrated model of engulfment duration. J Theor Biol. 267:437–453.

Ramp C, Delarue J, Palsbøll PJ, Sears R, Hammond PS. 2015. Adapting to a warmer ocean - Seasonal shift of baleen whale movements over three decades. PLoS One 10(3):e0121374.

Rasband W. 2012. ImageJ. U S Natl Institutes Heal Bethesda, Maryland, USA.://imagej.nih.gov/ij/.

Rasmussen M. 2009. Whales in Skjálfandi Bay. Enviromental Impact Assess reports Krafla Power Station Bakki, Iceland. Available from: http://www.alcoa.com/iceland/en/info_page/bakki.asp

Rattenborg NC, De La Iglesia HO, Kempenaers B, Lesku JA, Meerlo P, Scriba MF. 2017. Sleep research goes wild: New methods and approaches to investigate the ecology, evolution and functions of sleep. Philos Trans R Soc B Biol Sci. 372(1734):20160251.

Robbins, J Mattila, D.K. Palsboll P.J. Berube M. 1998. Asynchronous diving pairs of humpback whales: implications of a newly described behavior observed in the North Atlantic wintering grounds. In: Abstract of the World Marine Mammals Science Conferance. Monaco. p. 20–24.

Rus HA, editor. 2002. Marine mammal biology: An evolutionay approach. Blackwell Publishing.

Sakamoto KQ, Sato K, Ishizuka M, Watanuki Y, Takahashi A, Daunt F, Wanless S. 2009. Can ethograms be automatically generated using body acceleration data from free-ranging birds? PLoS One 4(4):e5379.

Sato K, Mitani Y, Cameron MF, Siniff DB, Naito Y. 2003. Factors affecting stroking patterns and body angle in diving Weddell seals under natural conditions. J Exp Biol. 206:1461–1470.

Sato K, Watanuki Y, Takahashi A, Miller PJOO, Tanaka H, Kawabe R, Ponganis PJ, Handrich Y, Akamatsu T, Watanabe Y, et al. 2007. Stroke frequency, but not swimming speed, is related to body size in free-ranging seabirds, pinnipeds and cetaceans. Proc Biol Sci. 274(1609):471–477.

Shiomi K, Narazaki T, Sato K, Shimatani K, Arai N, Ponganis PJ, Miyazaki N. 2010. Data-processing artefacts in three-dimensional dive path reconstruction from geomagnetic and acceleration data. Aquat Biol. 8(3):299–304.

Simon M, Johnson M, Madsen PT. 2012. Keeping momentum with a mouthful of water: behavior and kinematics of humpback whale lunge feeding. J Exp Biol. 215(21):3786–98.

Stephens DW, Brown JS, Ydenberg RC. 2007. Foraging. Behaviour and ecology. Chicago: University of Chicago Press.

Stephens DW, Krebs JR. 1986. Testing foraging models. In: Foraging Theory. New Jersey: Princeton University Press. p. 183–205.

Stevick PT, Neves MC, Johansen F, Engel MH, Judith A, Marcondes MCC, Carlson C. 2011. A quarter of a world away: Female humpback whale moves 10 000 km between breeding areas. Biol Lett. 7(2):299-302.

Tanaka H, Takagi Y, Naito Y. 2001. Swimming speeds and buoyancy compensation of migrating adult chum salmon *Oncorhynchus keta* revealed by speed/depth/acceleration data logger. J Exp Biol. 204:3895–3904.

Thompson D, Fedak M a. 2001. How long should a dive last? A simple model of foraging decisions by breath-hold divers in a patchy environment. Anim Behav. 61(2):287–296.

Tyson RB, Friedlaender AS, Nowacek DP. 2016. Does optimal foraging theory predict the foraging performance of a large air-breathing marine predator? Anim Behav. 116:223–235.

Valsecchi E, Hale P, Corkeron P, Amos W. 2002. Social structure in migrating humpback whales (*Megaptera novaeangliae*). Mol Ecol. 11(3):507-518.

Vennell R, Pease D, Wilson B. 2006. Wave drag on human swimmers. J Biomech. 39:664–671.

Visser F, Hartman KL, Rood EJJ, Hendriks AJE, Zult DB, Wolff WJ, Huisman J, Pierce GJ. 2011. Risso's dolphins alter daily resting pattern in response to whale watching at the Azores. Mar Mammal Sci. 27(2):366-381.

Vogel S. 1994. Life in moving fluids: The physical bilogy of flow. 2nd ed. New Jersey: Princeton University Press.

Ware C, Friedlaender AS, Nowacek DP. 2011. Shallow and deep lunge feeding of humpback whales in fjords of the West Antarctic Peninsula. Mar Mammal Sci. 27(3):587–605.

Watanabe YY, Ito M, Takahashi A, Watanabe YY, Ito M, Takahashi A. 2014. Testing optimal foraging theory in a penguin − krill system Testing optimal foraging theory in a penguin – krill system. Proc R Soc B Biol Sci. 281(1779).

Watts DP. 1988. Environmental influences on mountain gorilla time budgets. Am J Primatol. 15(3):195-211.

Weinrich M, Nowacek D, Wiley D, Halpin P, Ware C, Hazen E, Friedlaender A, Hurst T. 2009. Diel changes in humpback whale *Megaptera novaeangliae* feeding behavior in response to sand lance Ammodytes spp. behavior and distribution. Mar Ecol Prog Ser. 395:91–100.

Weinrich MT. 1991. Stable social associations among humpback whales (*Megaptera novaeangliae*) in the southern Gulf of Maine. Can J Zool. 69(12): 3012-3019.

Werth AJ, Ford TJ. 2012. Abdominal fat pads act as control surfaces in lieu of dorsal fins in the beluga (*Delphinapterus*). Mar Mammal Sci. 28(4):E516-E527.

Whitehead H. 1983. Structure and stability of humpback whale groups off Newfoundland. Can J Zool. 61(6):1391-1397.

Williams TM, Friedl WA, Haun JE. 1993. The physiology of bottlenose dolphins (*Tursiops truncatus*): heart rate, metabolic rate and plasma lactate concentration during exercise. J Exp Biol. 179:31–46.

Williams TM, Haun JE, Friedl WA. 1999. The diving physiology of bottlenose dolphins (*Tursiops truncatus*). I. Balancing the demands of exercise for energy conservation at depth. J Exp Biol. 202:2739–2748.

Williams TM, Kooyman GL. 1985. Swimming performance and hydrodynamic characteristics of harbor seals *Phoca vitulina*. Physiol Zool. 58(5):576-589.

Woodward BL, Winn JP, Fish FE. 2006. Morphological specializations of baleen whales associated with hydrodynamic performance and ecological niche. J Morphol. 267(11):1284–1294.

Wright AJ, Akamatsu T, Mouritsen KN, Sveegaard S, Dietz R, Teilmann J. 2016. Review of low-level bioacoustic behavior in wild cetaceans: Conservation implications of possible sleeping behavior. In: Advances in Experimental Medicine and Biology.New York, Springer. p.1251-1258.

Zar JH. 1999. Biostatistical analysis, 4th Edition. Upper Saddle River, New Jersey: Prentace-Hall, Inc.

Zepelin H, Siegel JM, Tobler I. 2005. Mammalian Sleep. In: Principles and practice of sleep medicine. 4: 91-100

Acknowledgements

I would like to express my sincere gratitude to my supervisor Dr. Katsufumi Sato for his support and guidance throughout my research. Besides my advisor, I would particularly like to thank Dr. Kagari Aoki for all the thoughtful advices on my research and manuscripts. I cannot express enough thanks to the staffs of Minamichita Beachland Aquariam, Mr. Kenji Kuroyanagi for giving me the opportunity to do the experiment at the aquarium as well as comments on my research. Mr. Yoshio Matsuda and Ms. Natsuko Sakurai for taking the time out of their busy schedule to train the dolphins and carry out the experiments, and all the trainers for the support and help. My research could not have been accomplished without the encouragement and support of Dr. Tomonari Akamatsu from National Research Institute of Fisheries Science, for allowing me to join the research at Iceland. I would like to offer my special thanks to Dr. Marianne Helene Rasmussen and Dr. Maria Iversen from University of Iceland for also allowing me to work at Iceland and meaningful advice on my research. I would like to thank North Sailing whale-watching and Gentle Giants whale-watching for lending us their zodiac. I acknowledge Takashi Iwata for field assistance and advices on my research. I received generous support from Hiraku Konno of Observational Research Support Section upon making the tags and lending me tools. I would like to show my greatest gratitude to Dr. Patrick J.O. Miller from University of St Andrews, for sharing me large dataset of humpback whales in Norway and Canada as well as allowing me to join the research in Norway. I would like to express my great appreciation to all members in my laboratory, I would not have made it through this thesis without everyone's daily help and support. I would like to express my greatest appreciations to Dr. Shingo Kimura, Dr. Maki Suzuki, Dr. Yoshihisa Mori and Dr. Tomonari Akamatsu who reviewed this thesis and gave me thoughtful advices to improve my thesis. And last but not the least, I would like to thank my family for their support throughout my life.